

¹ Increasing prevalence of plant-fungal symbiosis across two
² centuries of environmental change

³ Joshua C. Fowler^{1,2*}

Jacob Moutouama^{1,3}

Tom E. X. Miller¹

⁴ 1. Rice University, Department of BioSciences, Houston, Texas 77006; 2. University of Miami,
⁵ Department of Biology, Miami, Florida; 3. Department of Botany, University of British Columbia,
⁶ 6270 University Blvd, Vancouver, BC V6T 1Z4

⁷ * Corresponding author; e-mail:jcf221@miami.edu

⁸ *Manuscript elements:* Figure 1 - Figure 6, Appendix A (including Figure A1 - Figure A15, Table
⁹ A1, and Supporting Methods).

¹⁰ *Keywords:* climate change, *Epichloë*, herbarium, INLA, museum specimen, plant-microbe sym-
¹¹ biosis, Poaceae, spatially-varying coefficients model

¹² *Running Title:* Increasing prevalence of *Epichloë* endophytes

¹³ *Manuscript type:* Research Article.

Abstract

Species' distributions and abundances are shifting in response to ongoing global climate change. Mutualistic microbial symbionts can provide hosts with protection from environmental stress that may promote resilience under environmental change, however this change may also disrupt species interactions and lead to declines in hosts and/or symbionts. Symbionts preserved within natural history specimens offer a unique opportunity to quantify changes in microbial symbiosis across broad temporal and spatial scales. We asked how the prevalence of seed-transmitted fungal symbionts of grasses (*Epichloë* endophytes) has changed over time in response to climate change, and how these changes vary across host species' distributions. Specifically, we examined 2,346 herbarium specimens of three grass host species (*Agrostis hyemalis*, *Agrostis perennans*, *Elymus virginicus*) collected over the past two centuries (1824 – 2019) for the presence or absence of *Epichloë* symbiosis. Analysis of an approximate Bayesian spatially-varying coefficients model revealed that endophytes increased in prevalence over the last two centuries from ca. 25% to ca. 75% prevalence, on average, across three host species. Changes in seasonal climate drivers were associated with increasing endophyte prevalence. Notably, increasing precipitation during the peak growing season for *Agrostis* species and decreasing precipitation for *E. virginicus* were associated with increasing endophyte prevalence. Changes in the variability of precipitation and temperature during off-peak seasons were also important predictors of increasing endophyte prevalence. Our model performed favorably in an out-of-sample predictive test with contemporary survey data from across 63 populations, a rare extra step in collections-based research. However, there was greater local-scale variability in endophyte prevalence in contemporary data compared to model predictions, suggesting new directions that could improve predictive accuracy. Our results provide novel evidence for a cryptic biological response to climate change that may contribute to the resilience of host-microbe symbiosis through fitness benefits to symbiotic hosts.

Introduction

39 Understanding how biotic interactions are altered by global change is a major goal of basic and
40 applied ecological research (Blois et al., 2013; Gilman et al., 2010). Documented responses to envi-
41 ronmental change, such as shifts in species' distributions (Aitken et al., 2008) and phenology (Piao
42 et al., 2019), are typically blind to concurrent changes in associated biotic interactions. Empirically
43 evaluating these biotic changes – whether interacting species shift in tandem with their partners
44 or not (HilleRisLambers et al., 2013) – is crucial to predicting the reorganization of Earth's biodi-
45 versity under global change. Such evaluations have been limited because few datasets on species
46 interactions extend over sufficiently long time scales of contemporary climate change (Poisot et al.,
47 2021).

48 Natural history specimens, which were originally collected to document and preserve taxonomic
49 diversity, present a unique opportunity to explore long-term changes in biodiversity and ecological
50 interactions across broad spatial and temporal scales (Davis, 2023; Meineke et al., 2018). Natural
51 history collections, built and maintained by the efforts of thousands of scientists, are invaluable
52 time machines, primarily comprised of physical specimens of organisms along with information
53 about the time and place of their collection. These specimens often preserve physical legacies
54 of ecological processes and species' interactions from dynamically changing environments across
55 time and space (Lendemer et al., 2020). For example, previous researchers have examined the
56 flowers, pollen grains, and leaves of specimens within plant collections (herbaria) to document shifts
57 in reproductive phenology (Berg et al., 2019; Park et al., 2019; Willis et al., 2017), pollination
58 (Duan et al., 2019; Pauw and Hawkins, 2011), and herbivory (Meineke et al., 2019) related to
59 anthropogenic climate change. Herbarium specimens have also been used to identify the origins
60 and population genomics of plant diseases such as *Phytophthora*, the Irish potato famine pathogen
61 (Ristaino et al., 2001; Ristaino, 2002; Yoshida et al., 2013), and have been proposed as vehicles
62 to track other emerging plant pathogens (Bradshaw et al., 2021; Ristaino, 2020). However, few
63 previous studies have leveraged biological collections to examine climate change-related shifts in a

64 particularly common type of interaction: mutualistic microbial symbiosis.

65 Microbial symbionts are common to all macroscopic organisms and can have important effects
66 on their hosts' survival, growth and reproduction (McFall-Ngai et al., 2013; Rodriguez et al., 2009).
67 Many microbial symbionts act as mutualists, engaging in reciprocally beneficial interactions with
68 their hosts in ways that can ameliorate environmental stress. For example, bacterial symbionts of
69 insects, such as *Wolbachia*, can improve their hosts' thermal tolerance (Reno et al., 2019; Truitt
70 et al., 2019), and arbuscular mycorrhizal fungi, documented in 70-90% of families of land plants
71 (Parniske, 2008), allow their hosts to persist through drought conditions by improving water and
72 nutrient uptake (Cheng et al., 2021). On the other hand, changes in the mean and variance of
73 environmental conditions may disrupt microbial mutualisms by changing the costs and benefits
74 of the interaction for each partner in ways that can cause the interaction to deteriorate (Aslan
75 et al., 2013; Fowler et al., 2024). Coral bleaching (the loss of symbiotic algae) due to temperature
76 stress (Sully et al., 2019) is perhaps the best known example, but this phenomenon is not unique
77 to corals. Lichens exposed to elevated temperatures experienced loss of photosynthetic function
78 along with changes in the composition of their algal symbiont community (Meyer et al., 2022).
79 How commonly and under what conditions microbial mutualisms deteriorate or strengthen under
80 climate change remain unanswered questions (Frederickson, 2017). Previous work suggests that
81 these alternative responses may depend on the intimacy and specialization of the interaction as well
82 as the physiological tolerances of the mutualist partners (Rafferty et al., 2015; Toby Kiers et al.,
83 2010; Warren and Bradford, 2014).

84 Understanding how microbial symbioses are affected by climate change is additionally compli-
85 cated by spatial heterogeneity in the direction and magnitude of environmental change (IPCC, 2021).
86 Beneficial symbionts are likely able to shield their hosts from environmental stress in locations that
87 experience a small degree of change, but symbionts in locations that experience changes of large
88 magnitude may be pushed beyond their physiological limits (Webster et al., 2008). Additionally,
89 symbionts are often unevenly distributed across their host's distribution. Facultative symbionts
90 may be absent from portions of the host range (Afkhami et al., 2014), and hosts may engage with

91 a diversity of partners (different symbiont species or locally-adapted strains) across environments
92 (Fowler et al., 2023; Fraude et al., 2008; Rolshausen et al., 2018). Identifying broader spatial trends
93 in symbiont prevalence is therefore an important step in developing predictions for where to expect
94 changes in the symbiosis in future climates.

95 *Epichloë* fungal endophytes are specialized symbionts of cool-season grasses, estimated from
96 surveys to associate with ~ 20 – 30% of species across the diverse Poaceae family (Leuchtmann,
97 1992). Within the cool-season grass subfamily (Pooideae), it has been estimated that between 17%
98 to 40% of sampled species act as *Epichloë* hosts (Card et al., 2014; Iannone et al., 2011). They
99 are predominantly transmitted vertically from maternal plants to offspring through seeds. Vertical
100 transmission creates a feedback between the fitness of host and symbiont (Douglas, 1998; Fine,
101 1975; Rudgers et al., 2009). Over time, endophytes that act as mutualists should rise in prevalence
102 within a host population, particularly under environmental conditions that elicit protective benefits
103 (Donald et al., 2021). *Epichloë* are known to improve their hosts' drought tolerance (Decunta et al.,
104 2021) and protect their hosts against herbivores (Ambrose et al., 2014; Crawford et al., 2010) and
105 pathogens (Tian et al., 2017; Xia et al., 2018) likely through the production of a suite of biologically
106 active molecules, including diverse alkaloids, proteins, and other secondary metabolites. The fitness
107 feedback induced by vertical transmission leads to the prediction that endophyte prevalence should
108 be high in populations where these fitness benefits are most important. Previous survey studies
109 of contemporary populations have documented large-scale spatial patterns in endophyte prevalence
110 structured by environmental gradients (Afkhami, 2012; Bazely et al., 2007; Granath et al., 2007;
111 Sneck et al., 2017). We predicted that endophyte prevalence should track temporal changes in
112 environmental drivers (i.e. drought) that elicit strong fitness benefits.

113 Early research on *Epichloë* used herbarium specimens to describe the broad taxonomic diversity
114 of grass host species that harbor these symbionts (White and Cole, 1985), establishing that endo-
115 phyte symbiosis could be identified in plant tissue from as early as 1851. However, no subsequent
116 studies, to our knowledge, have used the vast resources of biological collections to quantitatively
117 assess spatio-temporal trends in endophyte prevalence and their environmental correlates. Grasses

118 are commonly collected and identified based on the presence of their reproductive structures, mean-
119 ing that preserved specimens typically contain seeds, conveniently preserving the seed-transmitted
120 fungi along with their host plants on herbarium sheets. This creates the opportunity to leverage
121 the unique spatio-temporal sampling of herbarium collections to examine the response of this sym-
122 biosis to historical climate change. However, the predictive ability derived from historical analyses
123 is rarely tested against contemporary data (Lee et al., 2024). Critically evaluating whether insights
124 from historical reconstruction are predictive of variation across contemporary populations is a cru-
125 cial step for the field to move from reading signatures of the past to forecasting ecological dynamics
126 into the future.

127 In this study, we assessed the long-term responses of *Epichloë* endophyte symbiosis to climate
128 change through the use of herbarium specimens of three North American host grass species (*Agrostis*
129 *hyemalis*, *Agrostis perennans*, and *Elymus virginicus*). We first addressed questions describing
130 spatial and temporal trends in endophyte prevalence: (i) How has endophyte prevalence changed
131 over the past two centuries? and (ii) How spatially variable are temporal trends in endophyte
132 prevalence across eastern North America? We then addressed how climate change may be driving
133 trends in endophyte prevalence by asking: (iii) What is the relationship between temporal trends
134 in endophyte prevalence and associated changes in climate drivers? We predicted that overall
135 endophyte prevalence would increase over time in tandem with climate change, and that localized
136 hotspots of endophyte change would correspond spatially to hotspots of climate warming and drying.
137 Finally, we evaluated (iv) how our model, built on data from historic specimens, performed in an out-
138 of-sample test using data on endophyte prevalence from contemporary surveys of host populations.
139 To answer these questions we examined a total of 2,346 historic specimens collected across eastern
140 North America between 1824 and 2019, and evaluated model performance against contemporary
141 surveys comprising 1,442 individuals from 63 populations surveyed between 2013 and 2020.

Methods

Focal species

144 Our surveys focused on three native North American grasses: *Agrostis hyemalis*, *Agrostis perennans*,
145 and *Elymus virginicus* that host *Epichloë* symbionts. These cool-season grass species have broad
146 distributions covering much the eastern United States (Fig. 1) and are commonly represented in
147 natural history collections. Cool-season grasses grow during the cooler temperatures of spring and
148 autumn due to their reliance on *C*₃ photosynthesis. *A. hyemalis* is a small short-lived perennial
149 species that germinates in autumn to late winter winter and typically flowers between March and
150 July (most common collection month: May). *A. perennans* is of similar stature but is longer lived
151 than *Agrostis hyemalis* and flowers in late summer and early autumn (most common collection
152 month: September). *A. perennans* is more sparsely distributed, tending to be found in shadier and
153 moister habitats, while *A. hyemalis* is commonly found in open and recently disturbed habitats.
154 Both *Agrostis* species are recorded from throughout the Eastern US, but *A. perennans* has a slightly
155 more northern distribution, whereas *A. hyemalis* is found rarely as far north as Canada and is listed
156 as a rare plant in Minnesota. *E. virginicus* is a larger and longer-lived species that is more broadly
157 distributed than the *Agrostis* species. It begins flowering as early as March or April but continues
158 throughout the summer (most common collection month: July).

159 Both *Agrostis* species host *Epichloë amarillans* (Craven et al., 2001; Leuchtmann et al., 2014),
160 and *Elymus virginicus* typically hosts *Epichloë elymi* (Clay and Schardl, 2002). The fungal sym-
161 bionts primarily reproduce asexually and are passed from maternal plant to offspring by vertical
162 transmission through seeds. These symbionts are also capable of horizontal transmission between
163 hosts via the production of external reproductive structures, including sexual spore-bearing stro-
164 mata that grow over host inflorescences (known as 'choke disease') and epiphyllous conidia on leaf
165 surfaces that produce asexual spores (Tadych et al., 2014). Evidence suggests that production of
166 horizontal transmission structures by *Epichloë* occurs at low levels, and may be influenced by en-

167 vironmental and genotypic factors (Brem and Leuchtmann, 1999; Meijer and Leuchtmann, 2000;
168 Tintjer et al., 2008). In line with this, monitoring of long-term plots of *A. perennans* and *E. virginicus*
169 showed no production of stromata on *A. perennans* and on only less than 1% of *E. virginicus*
170 plants over 14 years (Fowler et al., 2024). A similar low frequency of stromata formation (only
171 0.37% of recorded inflorescences) was observed for *A. hyemalis* in a separate field experiment (Don-
172 ald et al., 2021). Some host species have shown the capacity to partner with multiple symbiont
173 species or strains, and in some cases multiple symbiont lineages can co-exist within a host popu-
174 lation (Mc Cargo et al., 2014). However, surveys have typically found limited *Epichloë* genotypic
175 diversity within host populations (Treindl et al., 2023). Across host populations, concentrations of
176 biologically-active biomolecules and the genes associated with their production vary substantially
177 (Schardl et al., 2012). In this analysis, we focus on the presence/absence of *Epichloë* symbionts,
178 and we discuss potential implications of symbiont genotypic diversity in the Discussion.

179 *Herbarium surveys*

180 We visited nine herbaria between 2019 and 2022 (see Table A1 for a summary of specimens included
181 from each collection). With permission from herbarium staff, we acquired seed samples from 1135
182 *A. hyemalis* specimens collected between 1824 and 2019, 357 *A. perennans* specimens collected
183 between 1863 and 2017, and 854 *E. virginicus* specimens collected between 1839 and 2019 (Fig. 1,
184 Fig. 2A, Fig. A1). We chose our focal species in part because they are commonly represented in
185 herbarium collections and produce many seeds, meaning that small samples would not diminish the
186 value of specimens for future studies. We collected 5-10 seeds per specimen after examining the
187 herbarium sheet under a dissecting microscope to ensure that we collected mature seeds, not florets
188 or unfilled seeds, fit for our purpose of identifying fungal endophytes with microscopy. We excluded
189 specimens for which information about the collection location and date were unavailable.

190 Each specimen was assigned geographic coordinates based on collection information recorded on
191 the herbarium sheet using the geocoding functionality of the *ggmap* R package (Kahle and Wickham,
192 2019). Many specimens had digitized collection information readily available, but for those that

193 did not, we transcribed information printed on the herbarium sheet. The identity of each specimen
194 collector was gathered as part of the sample's metadata. Collections were geo-referenced to the
195 nearest county centroid, or nearest municipality when that information was available. For fifteen
196 of the oldest specimens, only information at the state level was available, and so we used the state
197 centroid. The median pairwise distance between georeferenced coordinate points was 841 km. The
198 median longitudinal width of the bounding boxes generated to geocode municipality, county, or
199 state centroids was 44.7 km. Among those specimens geo-referenced at the state level, the largest
200 bounding box, spanning the state of Texas, was 1233 km wide. The smallest bounding boxes were
201 less than 1 km across for small municipalities (while this suggests high precision, we note that some
202 specimens were collected in natural habitat nearby to small municipalities not encompassed by these
203 bounding boxes).

204 Our visits focused on herbaria with historic strengths in grass collections (e.g. Texas A&M,
205 Missouri Botanic Garden) and other herbaria in the Southern Great Plains region of the United
206 States. While these nine herbaria garnered specimens that span the focal species' ranges, our dataset
207 unevenly samples across the study region (Fig. 1). Texas, Oklahoma, Louisiana, and Missouri are
208 the most represented states. Uneven sampling was most pronounced for *A. perennans*, which has
209 much of its range in the northeastern US. We explore the potential influence of spatial bias in
210 sampling on our results through a simulation analysis (Appendix A - Supporting Methods).

211 After collecting seed samples, we quantified the presence or absence of *Epichloë* fungal hyphae
212 in each specimen using microscopy. We first softened seeds with a 10% NaOH solution, then stained
213 the seeds with aniline blue-lactic acid stain and squashed them under a microscope cover slip. We
214 examined the squashed seeds for the presence of fungal hyphae at 200-400X magnification (Bacon
215 and White, 2018). On average we scored 4.7 intact seeds per specimen of *A. hyemalis*, 4.2 seeds
216 per specimen of *A. perennans*, and 3.8 seeds per specimen of *E. virginicus*; we scored 10,342 seeds
217 in total. Due to imperfect vertical transmission, the production of symbiont-free offspring from
218 symbiotic hosts (Afkhami and Rudgers, 2008), it is possible that symbiotic host-plants produce a
219 mixture of symbiotic and non-symbiotic seeds. We therefore designated a specimen as endophyte-

220 symbiotic if *Epichloë* hyphae were observed in one or more of its seeds, or non-symbiotic if *Epichloë*
221 hyphae were observed in none of its seeds. To capture uncertainty in the endophyte identification
222 process, we recorded both a "liberal" and a "conservative" endophyte score for each plant specimen.
223 When we confidently identified endophytes within a specimen's seeds, we assigned matching liberal
224 and conservative scores. When we identified potential endophytes with unusual morphology, low
225 uptake of stain, or a small amount of fungal hyphae across the scored seeds, we recorded a positive
226 identification for the liberal score and a negative identification for the conservative score. We
227 recorded the identity of each scorer as part of the data collection process. 89% of scored plants
228 had matching liberal and conservative scores, reflecting high confidence in endophyte status. The
229 following analyses used the liberal status, however repeating all analyses with the conservative status
230 yielded qualitatively similar results (Fig. A8).

231 *Modeling spatial and temporal changes in endophyte prevalence*

232 We assessed spatial and temporal changes in endophyte prevalence across each host distribution,
233 quantifying the "global" temporal trends averaged across space, and then examining spatial hetero-
234 geneity in the direction and magnitude of endophyte change (hotspots and coldspots) across the spa-
235 tial extent of each host's distribution. To account for the spatial non-independence of geo-referenced
236 occurrences, we used an approximate Bayesian method, Integrated Nested Laplace Approximation
237 (INLA), to construct spatio-temporal models of endophyte prevalence. INLA provides a computa-
238 tionally efficient method of ascertaining parameter posterior distributions for certain models that
239 can be formulated as latent Gaussian Models (Rue et al., 2009). Many common statistical models,
240 including structured and unstructured mixed-effects models, can be represented as latent Gaussian
241 Models. We incorporated spatial heterogeneity into this analysis using spatially-structured intercept
242 and slope parameters implemented as stochastic partial differential equations (SPDE) to approxi-
243 mate a continuous spatial Gaussian process. This SPDE approach is a flexible method of smoothing
244 across space while explicitly accounting for spatial dependence between data-points (Bakka et al.,
245 2018; Lindgren et al., 2011). Fitting models with structured spatial effects is possible with MCMC

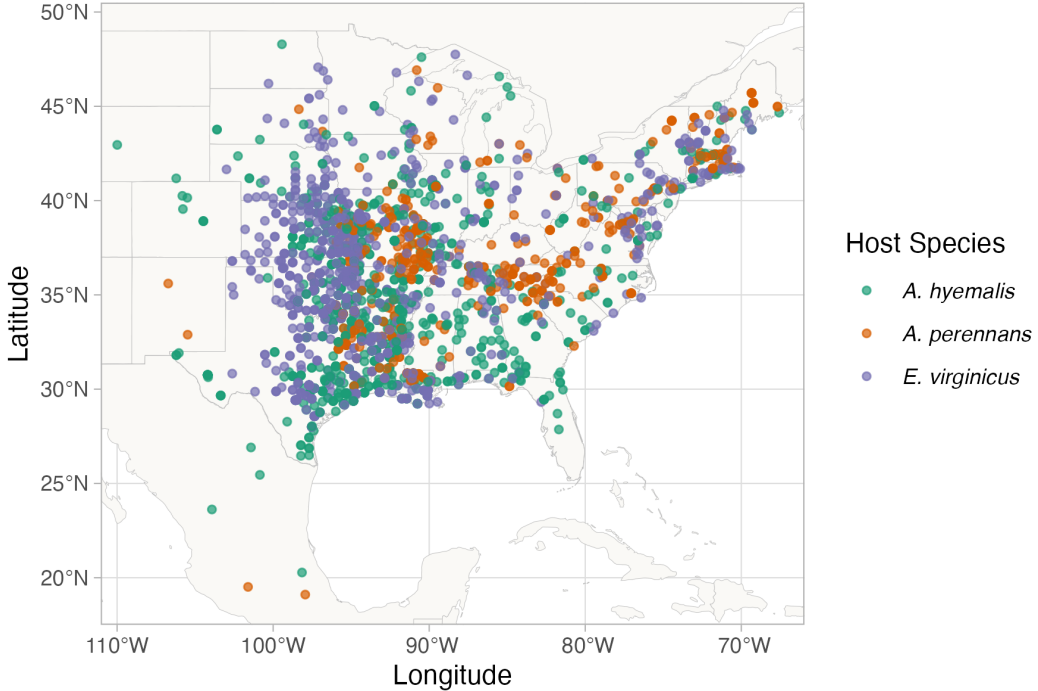


Figure 1: Collection locations of herbarium specimens sampled for *Epichloë* endophytes.

Specimens span eastern North America from nine herbaria, and are colored by host species (*A. hyemalis*: green, *A. perennans*: orange, *E. virginicus*: purple). Map lines delineate study areas and do not necessarily depict accepted national boundaries.

246 sampling but can require long computation times, making INLA an effective alternative. This ap-
 247 proach has been used to model spatial patterns in flowering phenology (Willems et al., 2022), the
 248 abundance of birds (Meehan et al., 2019) and butterflies (Crossley et al., 2022), the distribution of
 249 temperate trees (Engel et al., 2022) as well as the population dynamics of endangered amphibians
 250 (Knapp et al., 2016) and other ecological processes (Beguin et al., 2012).

251 We estimated global and spatially-varying trends in endophyte prevalence using a joint-likelihood
 252 model. For each host species h , endophyte presence/absence of the i^{th} specimen ($P_{h,i}$) was modeled
 253 as a Bernoulli response variable with expected probability of endophyte occurrence $\hat{P}_{h,i}$. We modeled
 254 $\hat{P}_{h,i}$ as a linear function of collection year, with intercept A_h and slope T_h defining the global
 255 temporal trend in endophyte prevalence specific to each host species as well as with spatially-

256 varying intercepts α_{h,l_i} and slopes τ_{h,l_i} associated with location (l_i , the unique latitude-longitude
 257 combination of the i th observation). The joint-model structure allowed us to “borrow information”
 258 across species in the estimation of shared variance terms for the spatially-dependent random effect
 259 δ_{l_i} , intended to account for residual spatial variation, and χ_{c_i} and ω_{s_i} , the i.i.d.-random effects
 260 indexed for each collector identity (c_i) and scorer identity (s_i) of the i^{th} specimen.

$$\text{logit}(\hat{P}_{h,i}) = A_h + T_h * \text{year}_i + \alpha_{h,l_i} + \tau_{h,l_i} * \text{year}_i + \delta_{l_i} + \chi_{c_i} + \omega_{s_i} \quad (1)$$

261 By including random effects for collectors and scorers, we accounted for “nuisance” variance that
 262 may bias predictions for changes in endophyte prevalence. Previous work suggests that behavior of
 263 historical botanists may introduce biases into ecological inferences made from historic collections
 264 (Kozlov et al., 2020). Prolific collectors who contribute thousands of specimens may be more or
 265 less likely to collect certain species, or specimens with certain traits (Daru et al., 2018). Similarly,
 266 the process of scoring seeds for hyphae involved multiple researchers (or "scorers") who, even with
 267 standardized training, may vary in their likelihood of positively identifying *Epichloë*.

268 We performed model fitting using the *inlabru* R package (Bachl et al., 2019). Global intercept
 269 and slope parameters, A and T , were given vague priors. Collector and scorer random effects, χ and
 270 ω respectively, were centered at 0 with precision parameters assigned penalized complexity (PC) pri-
 271 ors with parameter values $U_{PC} = 1$ and $a_{PC} = 0.01$ (Simpson et al., 2017). Each spatially-structured
 272 parameter depended on a covariance matrix according to the proximity of each pair of collection
 273 locations (Bakka et al., 2018; Lindgren et al., 2011). The covariance matrix was approximated using
 274 a Matérn covariance function, with each data point assigned a location according to the nodes of
 275 a mesh of non-overlapping triangles encompassing the study area (Fig. A2). Matérn covariance
 276 functions are widely used in spatially explicit statistical modeling because of their mathematical
 277 tractability and flexibility. This covariance structure relies on the assumption that the underlying
 278 process is stationary and isotropic, such that spatial autocorrelation between data points depends
 279 only on their relative positions (Bakka et al., 2018).

280 Implementing spatially-structured parameters in INLA with this SPDE approach is useful par-

ticularly because space is treated as a continuous variable, allowing the model to make efficient use
of the data and generate predictions across the entire study region. The SPDE approach is flexible
enough that it can capture smooth trends across space that are informed by the data rather than
by spatial regions chosen *a priori* by researchers. However this flexibility also invites the risk of
overfitting, as with other non-linear modeling approaches (Lapeyrolerie and Boettiger, 2023; Ra-
mampiandra et al., 2023; Ward et al., 2014). Priors for the Matérn covariance function, termed
“range” and “variance”, define how proximity effects decay with distance. The choice of priors for
these types of spatial models is an area of active research (Bakka et al., 2018; Simpson et al., 2017),
but another advantage of the INLA approach is that its computational efficiency allows for prior
sensitivity analyses. Results presented in the main text reflect a prior range of 342 kilometers (i.e.
a 50% probability of estimating a range less than 342 kilometers). We tested a range of values
(from 68 kilometers to 1714 kilometers) and meshes (presented in the Supporting Methods – *Mesh*
and Prior Sensitivity Analysis), finding that while the magnitude and uncertainty of effects varied,
model results were qualitatively similar, i.e. the same direction of effects across space. We assessed
model fit with visual posterior predictive checks (Fig. A3) and measurements of AUC (Figs. A4-
A5) (Gelman and Hill, 2006). Through results and discussion that follow, we refer to the model
described in this section as the “endophyte prevalence model”.

298 *Modeling distributions of host species*

299 The herbarium records did not encompass the entirety of each host species’ range. Therefore, we
300 used additional data sources to model the geographic distribution of each host species, with two
301 goals: (1) generate realistic maps on which we could project the predictions of the INLA model,
302 and (2) use the geographic distributions to test for relationships between climate change drivers and
303 trends in endophyte prevalence. We followed the ODMAP (overview, data, model, assessment,
304 prediction) protocol (Crossley et al., 2022) (see Supporting Methods). In short, we used presence-
305 only observations of each host species from Global Biodiversity Information Facility (GBIF) between
306 1990 to 2020 (713 occurrence records for *A. hyemalis* (GBIF.Org, 2025a), 656 occurrence records

307 for *A. perennans* (GBIF.Org, 2025b), and 2338 occurrence records for *E. virginicus* (GBIF.Org,
308 2025c)). We fit maximum entropy (MaxEnt) models using the maxent function in the R package
309 *dismo* (Hijmans et al., 2017) using the following seasonal climate predictors (1990-2020 climate
310 normals): mean and standard deviation of spring, summer, and autumn temperature, and mean
311 and standard deviation of spring, summer, and autumn cumulative precipitation.

312 We generated 10,000 pseudo-absences as background points, and split the occurrence data into
313 75% for model training and 25% for model testing. The performance of models was evaluated with
314 AUC (Jiménez-Valverde, 2012). We found AUC values of 0.862, 0.838, 0.821 respectively for *Agrostis*
315 *hyemalis*, *Agrostis perennans*, and *Elymus virginicus* indicating good model fit to data. We used
316 the training sensitivity (true positive rate) and specificity (true negative rate) to set a threshold for
317 transforming the continuous predicted probabilities into binary presence - absence host distribution
318 maps on which we projected INLA predictions of endophyte prevalence (Liu et al., 2005).

319 *Assessing the role of climate drivers*

320 We assessed how the magnitude of climate change may have driven changes in endophyte prevalence
321 by assessing correlations between changes in climate and changes in endophyte prevalence predicted
322 from our spatial model at evenly spaced pixels across the study area.

323 We first downloaded monthly temperature and precipitation rasters from the PRISM climate
324 group (Daly and Bryant, 2013) covering the time period between 1895 and 2020 using the *prism*
325 R package (Hart and Bell, 2015). PRISM provides reconstructions of historic climate variables
326 across the United States by spatially interpolating weather station data (Di Luzio et al., 2008).
327 Because the magnitude of observed climate change differs across seasons, and because different
328 growing seasons is a key feature of the biology of our focal host species, we calculated 30-year
329 climate normals for seasonal mean temperature and cumulative precipitation for the recent (1990
330 to 2020) and historic (1895 to 1925) periods. We used three four-month seasons within the year
331 (Spring: January, February, March, April; Summer: May, June, July, August; Autumn: September,
332 October, November, December). This division of seasons allowed us to quantify differences in

the primary climate change drivers, temperature and precipitation, associated with the two “cool” seasons, when we expected our focal species to be most active (*A. hyemalis* flowering phenology: spring; *E. virginicus*: spring and summer; *A. perennans*: autumn). In addition to mean climate conditions, environmental variability itself can influence population dynamics (Tuljapurkar, 1982) and changes in variability are a key prediction of climate change models (IPCC, 2021; Stocker et al., 2013). Therefore, we calculated the standard deviation for each annual and seasonal climate driver across each 30-year period. We then took the difference between recent and historic periods for the mean and standard deviation for each climate driver (Figs. A13-A15). All together, we assessed twelve potential climate drivers: the mean and standard deviation of spring, summer, and autumn temperature, as well as the mean and standard deviation of spring, summer, and autumn cumulative precipitation (the same climate covariates used in the MaxEnt models).

We then evaluated whether areas that have experienced the greatest changes in endophyte prevalence (hotspots of endophyte change) are associated with high degrees of change in climate (hotspots of climate change). To do so, we modeled the fitted, spatially-varying slopes of endophyte change through time ($\tau_{h,l}$) as a linear function of environmental covariates, with a Gaussian error distribution for a set of pixels across each host distribution. The continuous SPDE approach taken from our endophyte prevalence model allows us to generate predictions of temporal trends in prevalence at arbitrarily many pixels across each host distribution. Balancing computation time with resolution, we generated predicted trends for 546, 645, and 753 pixels across each host distribution for *A. perennans*, *A. hyemalis*, and *E. virginicus* respectively (pixel dimensions: *A. perennans* = 65 km x 36 km; *A. hyemalis* = 61km x 45 km; *E. virginicus* = 62 km x 40 km). Fitting regressions to many pixels across the study region risks artificially inflating confidence in our results due to large sample sizes, and so we performed this analysis using only a random subsample of 250 pixels across the study region; other sizes of subsample yielded similar results. Data from each host species were analyzed separately. Throughout the results and discussion that follow, we refer to this analysis as the “*post hoc* climate regression analysis”.

359 *Validating model performance with in-sample and out-of-sample tests*

360 We evaluated the predictive ability of the endophyte prevalence model using both in-sample training
361 data from the herbarium surveys, and with out-of-sample test data, an important but rarely used
362 strategy in ecological studies (Lee et al., 2024; Tredennick et al., 2021). We generated out-of-
363 sample test data from contemporary surveys of endophyte prevalence in natural populations of *A.*
364 *hyemalis* and *E. virginicus* in Texas and the southern US. Surveys of *E. virginicus* were conducted
365 in 2013 as described in Sneck et al. (2017), and surveys of *A. hyemalis* took place between 2015
366 and 2020. Population surveys of *A. hyemalis* were initially designed to cover longitudinal variation
367 in endophyte prevalence towards its range edge, while surveys of *E. virginicus* were designed to
368 cover latitudinal variation. In total, we visited 43 populations of *A. hyemalis* and 20 populations
369 of *E. virginicus* across the south-central US, with emphasis on Texas and neighboring states (Fig
370 A12). number of plants sampled per population: 22.9); note that this sampling design provided
371 greater local depth of information than the herbarium records, where only one plant was sampled at
372 each locality. We quantified the endophyte status of each individual with microscopy as described
373 for the herbarium surveys (with 5-10 seeds scored per individual), and calculated the prevalence
374 of endophytes within the population (proportion of plants that were endophyte-symbiotic). For
375 each population, we compared the observed fraction of endophyte-symbiotic hosts to the predicted
376 probability of endophyte occurrence \hat{P} derived from the model for that location and year. The
377 contemporary survey period (2013-2020) is at the most recent edge of the time period encompassed
378 by the historical specimens used for model fitting.

379 **Results**

380 *How has endophyte prevalence changed over time?*

381 Across more than 2300 herbarium specimens dating back to 1824, we found that prevalence of
382 *Epichloë* endophytes increased over the last two centuries for all three grass host species (Fig. 2).

383 On average, endophytes of *A. perennans* and *E. virginicus* increased from ~ 40 % to 70% prevalence
384 across the study region, and *A. hyemalis* increased from ~ 25% to over 50% prevalence. Our model
385 indicates high confidence that overall temporal trends are positive across species (99% probability
386 of a positive overall year slope in *A. hyemalis*, 92% probability of a positive overall year slope in *A.*
387 *perennans*, and 91% probability of a positive overall year slope in *E. virginicus*) (Fig. A6).

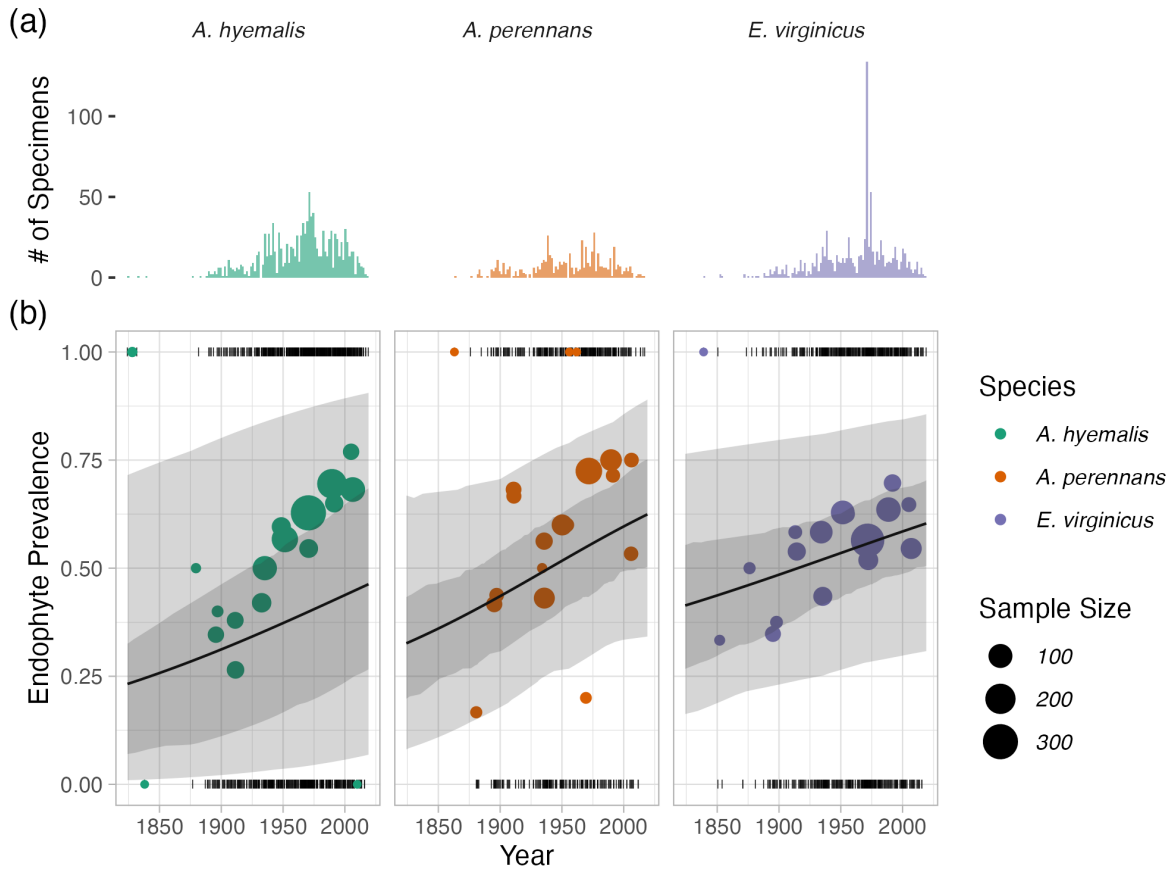


Figure 2: **Temporal trends in endophyte prevalence.** (A) Histograms show the frequency of scored specimens through time for each host species. (B) Lines show mean endophyte prevalence predicted by the endophyte prevalence model over the study period along with the 50% and 95% CI bands incorporating parameter uncertainty and variation associated with collector and scorer random effects. Colored points are binned means of the observed endophyte presence/absence data (black dashes). Colors represent each host species (*A. hyemalis*: green, *A. perennans*: orange, *E. virginicus*: purple) and point size represents the number of specimens.

388 The model appears to under-predict the observed increase in endophyte prevalence relative to
 389 the data, particularly for *A. hyemalis* (Fig. 2B), but the model is accounting for random effects
 390 and spatial non-independence that are not readily seen in the figure. We found no evidence that
 391 collector biases influenced our results. Collector random effects were consistently small (Fig. A9),

392 and models fit with and without this random effect provide qualitatively similar results. The identity
393 of individual scorers, the researchers who identified endophyte status microscopically, did contribute
394 to observed patterns in endophyte prevalence. For example, 3 of the 25 scorers were significantly
395 more likely than average to assign positive endophyte status, as indicated by 95% credible intervals
396 greater than zero, while 4 of the 25 had 95% credible intervals below zero (Fig. A10).

397 *How spatially variable are temporal trends in endophyte prevalence?*

398 While there was an overall increase in endophyte prevalence, our model revealed hotspots and
399 coldspots of change across the host species' ranges, which are mapped in Fig. 3 across geographic
400 ranges predicted by MaxEnt species distribution models. In some regions, posterior mean estimates
401 of spatially varying temporal trends indicate that *A. hyemalis* and *A. perennans* experienced in-
402 creases in prevalence by as much as 2% per year over the study period. Posterior estimates of
403 uncertainty in spatially varying slopes indicate that these hotspots of change may have experienced
404 increases of up to 5% per year while declines in prevalence may be as great as -4% per year for
405 the *Agrostis* species. (Fig. A7) In contrast, *E. virginicus* experienced increases up to around 1%
406 per year, with uncertainty ranging between 3.5% increases and 2.5% decreases (Fig. A7) Taken
407 together, both *Agrostis* species show areas of both strong increasing and declining prevalence, while
408 *E. virginicus* had an overall weaker and geographically more homogeneous increase in endophyte
409 prevalence. Notably, endophytes are predicted to have increased most strongly towards the western
410 range edge of *A. hyemalis* (Fig. 3A) and across the northeastern US for *A. perennans* (Fig. 3B).
411 Broad increases in prevalence on average, along with increases towards range edges that had low
412 historic prevalence result in range expansions of the symbiosis for both *Agrostis* species (Fig. 4).
413 Increases in prevalence were strongest in regions with low historic prevalence for the *Agrostis* species
414 (Fig. A11 A-B), but for *E. virginicus* trends did not differ according to historic prevalence (A11
415 C).

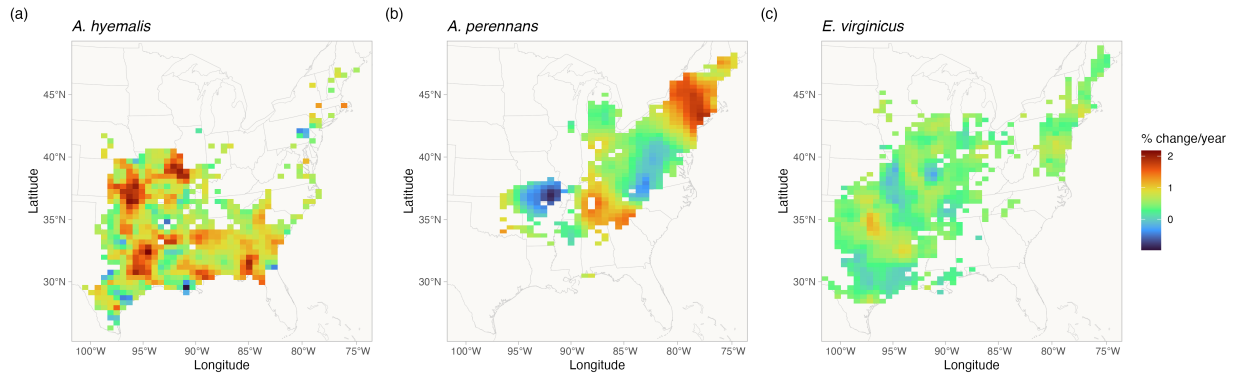


Figure 3: Predicted posterior mean of spatially-varying slopes representing change in endophyte prevalence for each host species ((A)*A. hyemalis*; (B)*A. perennans*; (C)*E. virginicus*). Spatially-varying trends are estimated from the endophyte prevalence model. Color indicates the relative change in predicted endophyte prevalence. Map lines delineate study areas and do not necessarily depict accepted national boundaries.

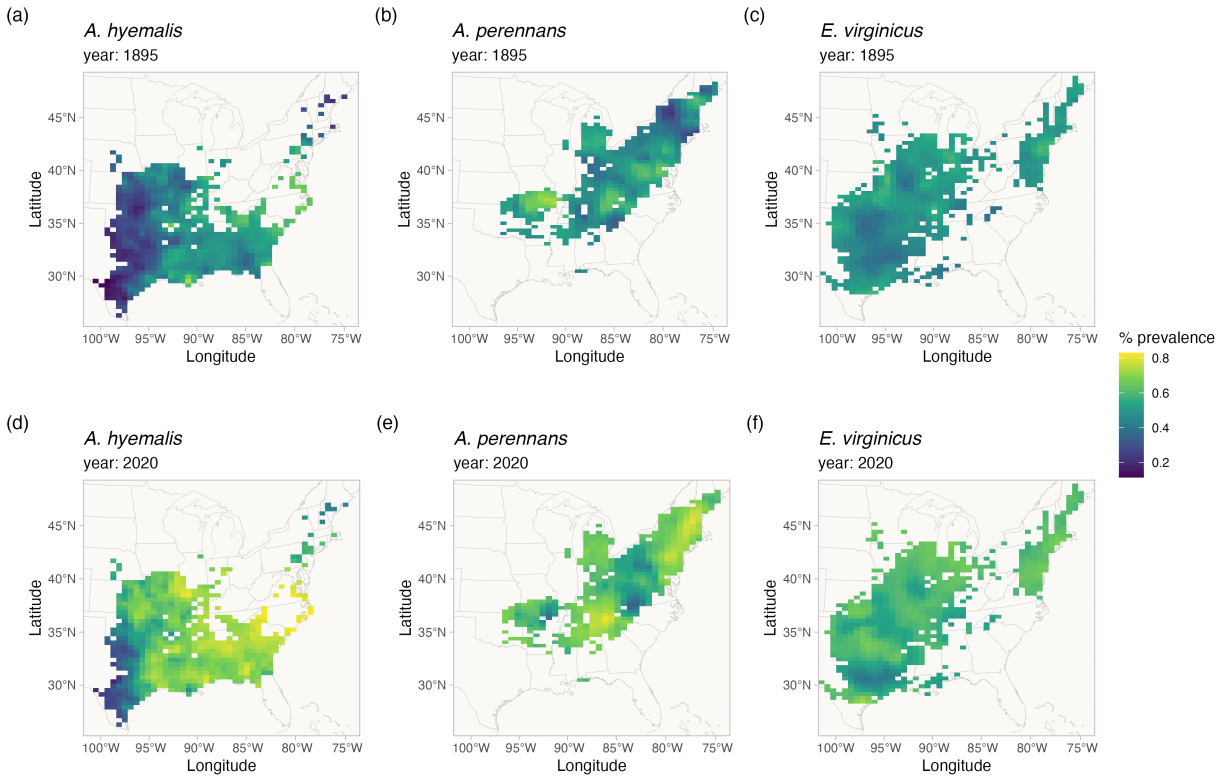


Figure 4: Predicted endophyte prevalence for each host species in 1895 and 2020. Predictions of prevalence come from the endophyte prevalence model. Color indicates the posterior mean endophyte prevalence for (A, D) *A. hyemalis*, (B, E) *A. perennans*, and (C, F) *E. virginicus*. Map lines delineate study areas and do not necessarily depict accepted national boundaries.

416 *What is the relationship between variation in temporal trends in endophyte
417 prevalence and changes in climate drivers?*

418 We found that trends in endophyte prevalence were strongly associated with one or more seasonal
419 climate change drivers (Fig. 5). For the majority of the study region, the climate has become
420 wetter (an average increase in annual precipitation of 60 mm) with relatively minimal temperature
421 warming (an average increase in annual temperature of 0.02 °C) over the last century (Fig. A13-
422 A15), a consequence of regional variation in global climate change (IPCC, 2021). Within the

423 region, climate changes were spatially variable; certain locations experienced increases in annual
424 precipitation as large as 375 mm or decreases up to 54 mm across the last century, while annual
425 temperature changes ranged from warming as great as 1.4 °C to cooling by 0.46 °C.

426 Spatially variable climate trends were predictive of trends in endophyte prevalence. For exam-
427 ple, among the tested climate drivers, strong increases in endophyte prevalence for *A. perennans*
428 were most strongly associated with increasing autumn precipitation and with increasing mean and
429 variability in autumn temperature (greater than 97% posterior probabilities of positive slopes). For
430 this species, each 1 °C increase in autumn temperature was associated with a 1.07 % greater increase
431 per year in endophyte prevalence (Fig. 5A) and a 100 mm increase in precipitation was associated
432 with a 0.8% greater increase per year in endophyte prevalence (Fig. 5B). This result aligns with
433 the species' autumn active growing season, however other seasonal climate drivers were also posi-
434 tively associated with increasing endophyte prevalence in this host species. In particular, we found
435 cooler and drier springs and cooler summers to be associated with increasing endophyte prevalence
436 (greater than 99% posterior probabilities of negative slopes), though these slopes were generally of
437 smaller magnitude than those for autumn climate drivers. Changes in endophyte prevalence across
438 the ranges of *A. hyemalis* and *E. virginicus* were less strongly driven by changes in climate. Like
439 *A. perennans*, climate during peak growing season (spring for *A. perennans* and summer for *E. vir-*
440 *ginicus*) emerged most commonly as drivers of changes in endophyte prevalence. Across the tested
441 climate drivers, increases in mean spring precipitation were the strongest predictor of increasing
442 trends in endophyte prevalence for *A. hyemalis* (Fig. 5B) (greater than 99% posterior probability
443 of a positive slope). For this species, an increase of 100 mm in spring precipitation was associated
444 with 0.6% per year stronger increases in endophyte prevalence relative to regions with no change in
445 precipitation. The next greatest slopes were those associated with variability in spring precipitation
446 (greater than 96% posterior probability of a negative slope), as well as in the mean and variabil-
447 ity of autumn climate (greater than 98% probability of negative and positive slopes, respectively).
448 Changes in endophyte prevalence in *E. virginicus* were not strongly associated with changes in most
449 climate drivers, but regions with reduced variability in autumn precipitation (Fig. 5B) and with

450 cooler and more variable summer temperatures (Fig. 5A,C) experienced the largest increases in
451 endophyte prevalence. Our analysis indicated relatively high confidence that these climate drivers
452 influence endophyte prevalence shifts in *E. virginicus* (greater than 99% posterior probability of ei-
453 ther negative or positive slopes respectively), however they translate, for example, to less than a
454 0.4% decrease in endophyte prevalence per year for each $1^{\circ}C$ of summer warming over the century.
455 Repeating this analysis using all pixels across each species' distribution were qualitatively similar
456 to these results.

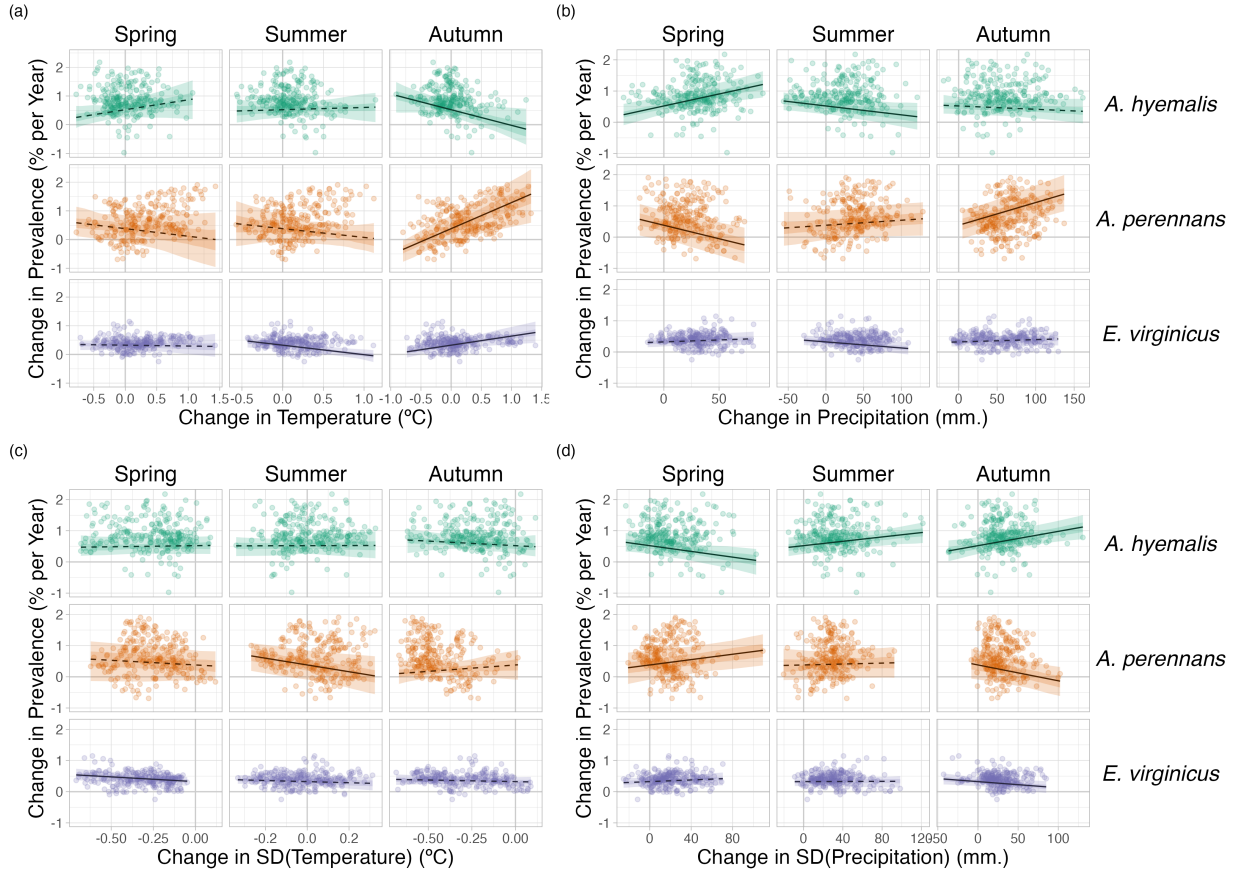


Figure 5: Relationships between predicted trends in endophyte prevalence and changes in seasonal climate drivers. Lines show marginal predicted relationship between spatially-varying trends in endophyte prevalence and changes in mean and variability of climate ((A): mean temperature, (B): cumulative precipitation, (C): standard deviation in temperature, (D): standard deviation in precipitation) estimated from the *post hoc* climate regression analysis. Confidence bands represent the 50 and 95% CI, colored by host species (*A. hyemalis*: green, *A. perennans*: orange, *E. virginicus*: purple). Slopes with greater than 95% posterior probability of being either positive or negative are represented as solid lines while those that have less than 95% probability are dashed. Points are the values of pre-computed SVC trends and climate drivers at 250 randomly sampled pixels across each host's distribution used in model fitting for the *post hoc* climate regression analysis.

457 *Evaluation of model performance on an out-of-sample test*

458 Tests of the endophyte prevalence model's predictive performance, as quantified by AUC and by
459 visual posterior predictive checks, indicated good predictive ability. Model performance was similar
460 between historic herbarium specimens used as training data and the out-of-sample test data from
461 contemporary surveys (AUC = 0.79 and 0.77 respectively; Fig. A5-A4). The model successfully
462 captured broad regional trends in endophyte prevalence seen in the contemporary survey data,
463 such as decline endophyte prevalence in *A. hyemalis* towards western longitudes (Fig. 6A) and an
464 increase towards northern latitudes (Fig. 6B). It is noteable that model predictions for endophyte
465 prevalence exhibited relatively little local geographic variation, whereas the out-of-sample survey
466 data were highly variable with populations spanning 0% to 100% endophyte-symbiotic plants (Fig.
467 6C), indicating population-to-population variation not captured in the endophyte prevalence model.

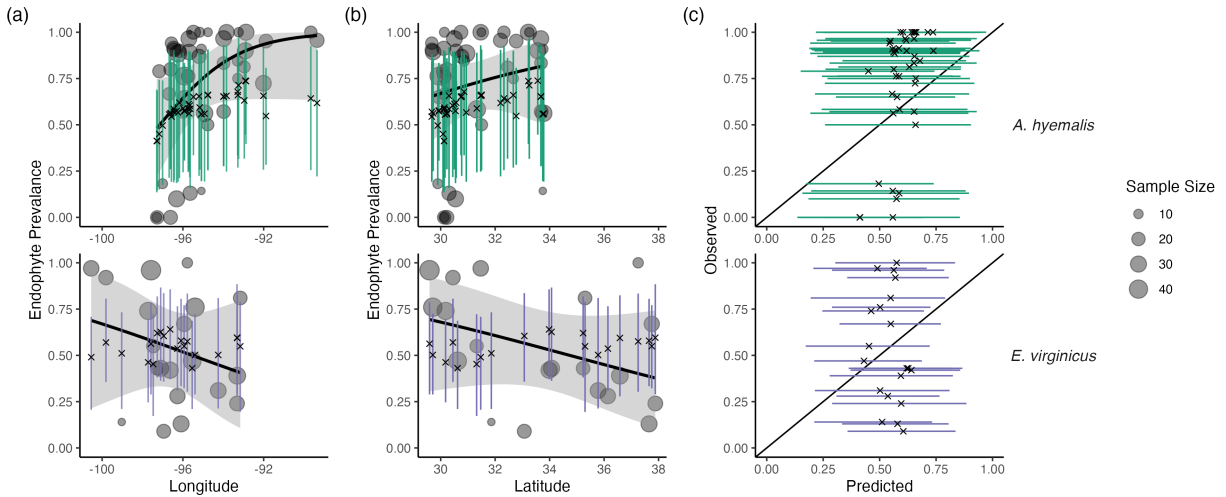


Figure 6: **Predictive performance for contemporary test data.** (A) The endophyte prevalence model, trained on historic herbarium collection data, performed modestly at predicting prevalence in contemporary population surveys. The model captured regional trends across (A) longitude and (B) latitude. Crosses indicate predicted mean prevalence along with the 95% CI (colored lines: *A. hyemalis*: green, orange, *E. virginicus*: purple) from the herbarium model. Contemporary prevalence is represented by grey points (point size reflects sample size) along with trend lines from generalized linear models (black line and shaded 95% confidence interval). (C) Comparison of contemporary observed population prevalence vs. predicted endophyte prevalence shows that contemporary test data had more variance between populations than in model predictions.

Discussion

Our examination of historic plant specimens revealed previously hidden shifts in microbial symbiosis over the last two centuries. For the three grass host species we examined, there have been strong increases in prevalence of *Epichloë* endophyte symbiosis. We interpret increases in prevalence of *Epichloë*, which are predominantly vertically transmitted, as adaptive changes that improve the fitness of their hosts under increasing environmental stress. This interpretation is in line with theory predicting that positive fitness feedback caused by vertical transmission leads beneficial symbionts

475 to rise in prevalence within a population (Donald et al., 2021; Fine, 1975). We further found that
476 trends in endophyte prevalence often varied across the host distribution in association with changes
477 in climate drivers, consistent with the hypothesis that increases in endophyte prevalence are driven
478 by context-dependent benefits to hosts that confer resilience under environmental change. Taken
479 together, our results suggest an overall strengthening of host-symbiont mutualism over the last two
480 centuries.

481 *Responses of host-microbe symbioses to climate change*

482 Differences across host species underscore that while all of these C_3 grasses share similar broad-scale
483 distributions, each engages in unique biotic interactions and has unique responses to environmental
484 drivers. We identified hotspots of change for *A. perennans*, which was the species whose endophyte
485 prevalence was most responsive to changes in climate drivers (Fig. 5). Predicted declines of 0.9%
486 per year in the southern portion of its range and predicted increases of up to 2% per year in the
487 north suggest a potential poleward range shift of endophyte-symbiotic plants (Fig. 3B); whether
488 the overall host distribution is shifting in parallel is an exciting next question.

489 Based on previous work demonstrating that endophytes can shield their hosts from drought
490 stress (reviewed in Decunta et al. (2021)), we generally predicted that drought conditions would be
491 a driver of increasing endophyte prevalence. In contrast to this expectation, increasing prevalence
492 for *A. perennans* was associated with both increasing autumn temperature and precipitation (Fig.
493 5). To our knowledge, the response of the symbiosis in *A. perennans* to drought has not been
494 examined experimentally, but in a greenhouse experiment, endophytes had a positive effect on host
495 reproduction under shaded, low-light conditions (Davitt et al., 2010). Our results also hint that it
496 may be useful to investigate whether lagged climate effects are important predictors of host fitness
497 in this system (Evers et al., 2021). Endophyte prevalence of the autumn-flowering *A. perennans* was
498 strongly linked with decreasing spring precipitation, and that of the spring-flowering *A. hyemalis*
499 was associated with decreasing autumn precipitation (Fig. 5B). For *A. hyemalis*, endophytes could
500 be playing a role helping hosts weather autumn-season droughts, which is likely also an important

time for the species' germination. Previous work demonstrated drought benefits in a greenhouse manipulation with this host-symbiont pair (Davitt et al., 2011), and early life stages may be particularly vulnerable to prolonged droughts. For *E. virginicus*, which experienced the weakest changes in endophyte prevalence overall (ranging between 1.1% increases and 0.2% decreases), we only found modest associations with changes in climate drivers. Surveys by Sneck et al. (2017), used as part of the test data in this study, identified a drought index (SPEI) that integrates precipitation with estimated evapotranspiration as an important predictor of contemporary endophyte prevalence in this species. The diverse relationships we detect between trends in endophyte prevalence and climate drivers suggest a more complicated picture than the simple explanation that drought alone, as measured through changes in annual precipitation, causes increasing endophyte prevalence through context-dependent fitness benefits.

While we show consistent increasing trends in prevalence between the three species, the mechanisms that explain these changes may be diverse and idiosyncratic. First, climate change responses may depend on genotype-specific responses that are not considered in our current analysis. While *Epichloë* symbioses are highly specialized, surveys have demonstrated genotypic and chemotypic diversity of the symbionts among and within populations (Treindl et al., 2023; von Cräutlein et al., 2021). Genotypic variation in *Epichloë* endophytes, particularly in genes responsible for alkaloid production, produces "chemotypes" with differing benefits for hosts against insect or mammalian herbivores mediated by environmental conditions (Ambrose et al., 2014; Saikkonen et al., 2013; Schardl et al., 2012). Genotypic variation of the hosts themselves can also influence interaction outcomes (Gundel et al., 2011a; Parker et al., 2017). Whether hotspots of change in endophyte prevalence reflect selection for genotype-pairings with particularly strong fitness benefits is an unanswered question. Additionally, *Epichloë* endophytes have been connected to a suite of non-drought related fitness benefits including herbivory defense (Brem and Leuchtmann, 2001), salinity resistance (Wang et al., 2020), and mediation of pathogens (Vikuk et al., 2019) and the soil microbiome (Roberts and Ferraro, 2015). Broad changes in the distribution and abundance of natural enemies (Côté et al., 2004), along with stresses from anthropogenic changes in land management and pollution (Sage,

528 2020) likely influence the benefits of symbiosis (Rudgers et al., 2020). Changing endophyte preva-
529 lence results from the combination of net fitness benefits playing out across the heterogeneous map
530 of a changing climate and and its interactive effects on other anthropogenic drivers. Host species
531 experience a world that is made increasingly stressful by a combination of global change drivers,
532 and while historic trends that we observed suggest that symbiotic fitness benefits have helped mit-
533 iate this stress, it is possible that at yet higher levels of stress, increasing costs of the mutualism
534 could lead to declines in endophyte prevalence. It is also known that stressful conditions can both
535 reduce (Gundel et al., 2011b) and increase (Gundel et al., 2020) the rate of successful transmission
536 of *Epichloë* endophytes from mother plant to offspring. These responses likely reflect both conse-
537 quences of host sanctions on costly symbionts and the ability of symbionts to successfully colonize
538 seeds (Afkhami and Rudgers, 2008; Gundel et al., 2011c). While we did not investigate differences
539 in the rate of transmission across these historic specimens due to low numbers of sampled seeds per
540 individual, it would be valuable to conduct deeper sampling for a subset of specimens with known
541 endophyte status and investigate how transmission itself may respond to environmental change. Ad-
542 ditionally, we have interpreted increasing prevalence as a signature of increased host fitness driven
543 by vertical transmission, which we expect is the predominant mode of tranmission in this system.
544 Horizontal transmission, while rare, could also explain increasing prevalence if global change stres-
545 sors lead symbionts to engage in increased parasitic behavior, resulting in increased dispersal and
546 transmission at the cost of host fitness. More extreme climate stresses, which are expected more
547 frequently in the future (Seneviratne et al., 2021) could shift the balance of interactions costs and
548 benefits. Identifying ‘tipping points’ of mutualism breakdown under increasing environmental stress
549 is an important area of future inquiry.

550 Our results indicate that *Epichloë* symbiosis has likely improved host fitness in stressful envi-
551 ronments leading to increasing prevalence. What is less clear is how this will influence future range
552 shifts. Based on our analysis, it is likely that the symbiosis will facilitate range shifts for hosts by
553 improving population growth at range edges. Previous population surveys (Rudgers and Swafford,
554 2009; Semmarin et al., 2015; Sneck et al., 2017) attributed environment-dependent gradients in

555 endophyte prevalence to symbiont-derived fitness benefit's allowing hosts to persist in environments
556 where they otherwise could not (Afkhami et al., 2014; Kazenel et al., 2015). However, symbiont-
557 facilitated range shifts require that endophytes be present in the populations to be able to contribute
558 to population growth. For example, the arid western range edge of *A. hyemalis* has had historically
559 low endophyte prevalence (Fig. 4), and dispersal of symbionts may limit the capacity for range
560 shifts. A range edge population with no endophytes would require dispersal of symbionts to oc-
561 cur, either via symbiotic seeds or horizontally-transmitted fungal spores, before the symbiosis could
562 result in an expanding distribution (Fowler et al., 2023). At the same time, we found that endo-
563 phyte prevalence has increased most quickly in regions with historically low endophyte prevalence
564 (Fig. A11), suggesting strong selection for symbiotic hosts when they are present. These factors
565 potentially contribute to the ability of the host species to track its environmental niche. Another
566 interesting question is the degree to which symbiotic and non-symbiotic hosts, which occupy over-
567 lapping but distinct niches, are likely to experience distribution shifts in tandem or at different rates
568 in the future.

569 *Steps towards forecasts of host-microbe symbioses*

570 The combination of a spatially-explicit model and historic herbarium specimens allowed us
571 to identify regions of both increasing and decreasing endophyte prevalence. We see several next
572 steps toward the goal of predicting host and symbiont niche-shifts in response to future climate
573 change. While the model successfully predicted large-scale spatial trends observed in the out-
574 of-sample contemporary population surveys, these data contained more population-to-population
575 variability in prevalence than could be explained by the model. We interpret this to mean that
576 the model captures coarse-scale spatial and temporal trends reasonably well, but is not equipped
577 to capture local-scale nuances that generate population-to-population differences. Validating our
578 model predictions with this test, a rare extra step in collections-based studies, allows us to identify
579 ways in which the model's out-of-sample predictive ability could be improved. Lack of information
580 on local variability in symbiont prevalence may simply be a feature of data derived from herbarium

581 specimens. Natural history collectors sample one or a few specimens from local populations, and
582 these observations are aggregated by the model to derive broad-scale estimates. This suggests that
583 increasing local replication should be a factor considered in future collection efforts of natural history
584 specimens, balancing the required time and effort along with limitations on storage space within
585 collections. Herbarium collections were predominately used for taxonomic research in the past,
586 but use of specimens to understand ongoing global change would benefit from increased collection
587 efforts and expansion of herbarium collections. An alternative validation test would be to hold-out
588 samples from the historic data set. Such a test would more clearly match the conditions of the
589 training data (i.e., in spatial scale and climate conditions), however the trade-off between training
590 and testing the model with a limited number of sampled specimens held us back from exploring this
591 option. Splitting datasets can negatively impact model estimates, and the choice of how to split
592 the data for model validation is not trivial (Bergmeir and Benítez, 2012; James et al., 2013).

593 Another key consideration in forecasting the dynamics of host-microbe symbioses is the spatial
594 scale of both specimen georeferencing and available climate data. For this analysis, most specimen
595 localities were assigned coordinates at county or city centroids, and the climate data examined
596 was on 4 km grid cells. Georeferencing of specimens as accurately as possible is a key priority
597 of herbarium specimen digitization efforts (Davis, 2023; Soltis, 2017). While the INLA modeling
598 approach that we used allows for predictions at arbitrarily small spatial scales, and would simplify
599 connecting model predictions to the scale of a given climate driver, the coarse scale inherent to our
600 analysis may obscure some local-scale ecological processes. Poor predictive ability at local scales in
601 this grass-endophyte system is not surprising, as previous studies have found that local variation
602 (e.g., in soil conditions, in microclimate), even to the scale of hundreds of meters can structure
603 endophyte-host niches (Gundel et al., 2024; Kazenel et al., 2015). Local adaptation in either the
604 host or symbiont to microclimate or soil conditions could cause populations to differ from broad
605 regional trends. The choice of prior distributions for spatially-varying random effects also impacts
606 the model's flexibility to capture spatial trends. Our exploration of model sensitivity to prior choice
607 (presented in the *Supplemental Methods*) reveals qualitatively similar results across a broad range

608 of priors. An important next step would be integrating data from local and regional scales through
609 modeling to constrain estimates of local and regional variation.

610 Predicting future niche-shifts of hosts and symbionts will require considering the coupled dynam-
611 ics of host-symbiont dispersal in addition to fitness benefits. For example, transplanting symbiotic
612 and non-symbiotic plants beyond the range edge of *A. hyemalis* could tell us whether low endophyte
613 prevalence in that area (Fig. 4A) is a result of environmental conditions that lead the symbiosis
614 to have negative fitness consequences, or is a result of some historical contingency or dispersal lim-
615 itation that has thus far limited the presence of symbiotic hosts from a region where they would
616 otherwise flourish and provide resilience. Incorporating available climatic and soil layers as covari-
617 ates is another obvious step that could improve predictions. These steps will bridge gaps that often
618 exist between large but broad bioclimatic and biodiversity data and small but high-resolution data
619 on biotic interactions, and move towards the goal of predicting the dynamics of microbial symbioses
620 under climate change (Isaac et al., 2020; Miller et al., 2019).

621 *Herbaria for global change research*

622 Our analysis advances the use of herbarium specimens in global change biology in two ways.
623 First and foremost, this is one of a growing number of studies to examine microbial symbiosis
624 using specimens from natural history collections, and the first, to our knowledge, to link long-term
625 changes in symbioses to changes in climate. The responses of microbial symbioses are a rich target
626 for future studies within historic specimens, particularly those that take advantage of advances
627 in sequencing technology. While we used relatively coarse presence/absence data based on fungal
628 morphology, other studies have examined historic plant microbiomes using molecular sequencing
629 and sophisticated bioinformatics techniques, but these studies have so far been limited to relatively
630 few specimens at limited spatial extents (Bearchell et al., 2005; Bieker et al., 2020; Bradshaw et al.,
631 2021, 2023; Gross et al., 2021; Heberling and Burke, 2019; Yoshida et al., 2015). Much of this work
632 highlights the important role that historic specimens can play in tracking pathogens, a particularly
633 important area as climate change facilitates the spread of new diseases (Ristaino, 2020; Singh et al.,
634 2023) Continued advances in capturing historic DNA and in filtering out potential contamination
635 during specimen storage (Bakker et al., 2020; Daru et al., 2019; Raxworthy and Smith, 2021) will
636 be imperative in the effort to scale up these efforts. This scaling up will be essential to be able
637 to quantify changes not just in the prevalence of symbionts, but also in symbionts' intraspecific
638 variation and evolutionary responses to climate change, as well as in changes in the wider host
639 microbiome. With improved molecular insights from historic specimens, we could ask whether
640 the broad increases in endophytes that we have identified reflect selection for particular genetic
641 strains or chemotypes and how this selection varies across space. Answering these questions as well
642 as the unknown questions that future researchers may ask also reiterates the value in capturing
643 meta-information during ongoing digitization efforts at herbaria around the world and during the
644 accession of newly collected specimens (Edwards et al.; Lendemer et al., 2020).

645 The second major advance in this analysis is in accounting for several potential biases in the data
646 observation process that may be common to many collections-based research questions by using a

647 spatially-explicit random effects model. Potential biases introduced by the sampling habits of col-
648 lectors (Daru et al., 2018), and variation between contemporary researchers during the collection of
649 trait data, if not corrected for could lead to over-confident inference about the strength and direction
650 of historic change (Fig. 2). Previous studies that have quantified the effects of collector biases typ-
651 ically find them to be small (Davis et al., 2015; Meineke et al., 2019), and we similarly did not find
652 that collector has a strong effect on the results of our analysis, but that scorer identity did impact
653 results. It is difficult to distinguish whether the impact of scorers was driven by true differences
654 in scorers' biases or by unintended spatial or temporal clustering of the specimens examined by
655 each scorer (Clayton et al., 1993; Urdangarin et al., 2023). By under-weighting endophyte-positive
656 samples that are clustered spatially or by collector or observer, the endophyte prevalence model is
657 appropriately accounting for nuisance variables and providing a conservative inference of endophyte
658 change relative to the raw data. Spatial autocorrelation is another phenomenon likely common
659 in data derived from herbarium specimens (Willems et al., 2022), which our spatially-explicit anal-
660 ysis models among samples. Beyond spatial autocorrelation of outcomes, systematic differences in
661 sampling across space can result in spatial bias.

662 One strength of herbaria as vehicles for global change research is the relative ease with which
663 specimens from many distinct geographic locations can be examined. We visited just nine institu-
664 tions in the central southern United States, and we were able to sample seeds from specimens across
665 an area spanning over 300,000 sq. km, including specimens from Mexico and Canada. Despite this
666 advantage, the specimens we examined are concentrated in the south-central United States, with
667 fewer specimens in the rapidly warming northeastern United States reflecting the regional focus of
668 herbaria. We provide a simulation analysis exploring the potential impact of spatially and tempo-
669 rally biased sampling (Appendix A - Supporting Methods). We found that the spatially-varying
670 coefficient model had a strong ability to re-capitulate temporal trends across space in simulated
671 data, and that this result was robust to relatively high levels of spatial bias (80% of data missing
672 from one spatial region). Simulation analyses that extend this work to consider the myriad ways
673 herbarium data may be biased (i.e. testing different spatial arrangements and scales of spatial

674 bias, or testing different sample sizes) would be extremely valuable (Daru et al., 2018; Erickson and
675 Smith, 2021; Gaul et al., 2020; Meineke and Daru, 2021; Schmidt et al.).

676 *Conclusion*

677 Ultimately, a central goal of global change biology is to generate predictive insights into the future of
678 natural systems on a rapidly changing planet. Beyond host-microbe symbioses, detecting ecological
679 responses to anthropogenic global change and attributing their causes would inform public policy
680 decision-makers and adaptive management strategies. Natural history specimens, such as the plant
681 hosts examined in this study, have a clear role to play in informing global change biodiversity
682 science, including building understanding of the dynamics of host-symbiont interactions (Davis,
683 2023). This survey of historic endophyte prevalence is necessarily correlative, yet it serves as a
684 foundation to develop better predictive models of the response of microbial symbioses to climate
685 change. Combining the insights from this type of regional-scale survey with field experiments and
686 physiological performance data could be invaluable to identify mechanisms driving shifts in host-
687 symbiont dynamics. Evidence is strong that certain dimensions of climate change correlated with
688 endophytes' temporal responses, however we do not know why trends in prevalence were weak
689 in some areas or how endophytes would respond to more extreme changes in climate. The "time
690 machine" of natural history collections revealed evidence of mutualism resilience for grass-endophyte
691 symbioses in the face of environmental change, but more extreme changes could potentially push
692 one or both partners beyond their physiological limits, leading to the collapse of the mutualism;
693 more research is needed to understand what those limits might be.

694 **Acknowledgments**

695 We thank Dr. Jessica Budke for help in drafting our initial destructive sampling plan, and to the
696 many staff members of herbaria who facilitated our research visits, as well as to the hundreds of
697 collectors who contributed to the natural history collections. Several high school and undergraduate
698 researchers contributed to data collection, including A. Appio-Riley, P. Bilderback, E. Chong, K.

699 Dickens, L. Dufresne, B. Gutierrez, A. Johnson, S. Linder, E. Scales, B. Scherick, K. Schrader, E.
700 Segal , G. Singla, and M. Tucker. This research was supported by funding from National Science
701 Foundation Division of Environmental Biology (grants 1754468 and 2208857) and by funding from
702 the Texas Ecolab Program. Five anonymous reviewers greatly improved earlier versions of this
703 manuscript.

704 **Statement of Authorship**

705 J.C.F. contributed to research conception, data collection, data analysis, and led manuscript draft-
706 ing. J.M. contributed to data analysis and manuscript revisions. T.E.X.M. contributed to research
707 conception, data collection, data analysis, and manuscript revisions.

708 **Data and Code Availability**

709 Data from this publication can be found through a publicly available repository
710 (<https://doi.org/10.5061/dryad.rn8pk0pn0>). Code for analyses can be found through a publicly
711 available repository (<https://github.com/joshuacfowler/EndoHerbarium>) that will be permanently
712 archived upon publication.

713

Literature Cited

- 714 M E Afkhami. Fungal endophyte–grass symbioses are rare in the California floristic province and
715 other regions with mediterranean-influenced climates. *Fungal Ecology*, 5(3):345–352, 2012.
- 716 M E Afkhami and J A Rudgers. Symbiosis lost: Imperfect vertical transmission of fungal endophytes
717 in grasses. *The American Naturalist*, 172(3):405–416, 2008.
- 718 M E Afkhami, P J McIntyre, and S Y Strauss. Mutualist-mediated effects on species’ range limits
719 across large geographic scales. *Ecology Letters*, 17(10):1265–1273, 2014.
- 720 S N Aitken, S Yeaman, J A Holliday, T Wang, and S Curtis-McLane. Adaptation, migration
721 or extirpation: Climate change outcomes for tree populations. *Evolutionary Applications*, 1(1):
722 95–111, 2008.
- 723 Karen V Ambrose, Albrecht M Koppenhöfer, and Faith C Belanger. Horizontal gene transfer of a
724 bacterial insect toxin gene into the epichloë fungal symbionts of grasses. *Scientific Reports*, 4(1):
725 5562, 2014.
- 726 C E Aslan, E S Zavaleta, B Tershy, and D Croll. Mutualism disruption threatens global plant
727 biodiversity: a systematic review. *PloS one*, 8(6):e66993, 2013.
- 728 F E Bachl, F Lindgren, D L Borchers, and J B Illian. inlabru: an R package for Bayesian spatial
729 modelling from ecological survey data. *Methods in Ecology and Evolution*, 10(6):760–766, 2019.
- 730 C W Bacon and J F White. Stains, media, and procedures for analyzing endophytes. In *Biotechnology
731 of endophytic fungi of grasses*, pages 47–56. CRC Press, 2018.
- 732 H Bakka, H Rue, G-A Fuglstad, A Riebler, D Bolin, J Illian, E Krainski, D Simpson, and F Lind-
733 gren. Spatial modeling with r-inla: A review. *Wiley Interdisciplinary Reviews: Computational
734 Statistics*, 10(6):e1443, 2018.

- 735 F T Bakker, V C Bieker, and M D Martin. Herbarium collection-based plant evolutionary genetics
736 and genomics. *Frontiers in Ecology and Evolution*, 8:603948, 2020.
- 737 D R Bazely, J P Ball, M Vicari, A J Tanentzap, M Bérenger, T Rakocevic, and S Koh. Broad-
738 scale geographic patterns in the distribution of vertically-transmitted, asexual endophytes in four
739 naturally-occurring grasses in sweden. *Ecography*, 30(3):367–374, 2007.
- 740 Sarah J Bearchell, Bart A Fraaije, Michael W Shaw, and Bruce DL Fitt. Wheat archive links long-
741 term fungal pathogen population dynamics to air pollution. *Proceedings of the National Academy
742 of Sciences*, 102(15):5438–5442, 2005.
- 743 J Beguin, S Martino, H Rue, and S G Cumming. Hierarchical analysis of spatially autocorrelated
744 ecological data using integrated nested laplace approximation. *Methods in Ecology and Evolution*,
745 3(5):921–929, 2012.
- 746 C S Berg, J L Brown, and J J Weber. An examination of climate-driven flowering-time shifts at
747 large spatial scales over 153 years in a common weedy annual. *American Journal of Botany*, 106
748 (11):1435–1443, 2019.
- 749 Christoph Bergmeir and José M Benítez. On the use of cross-validation for time series predictor
750 evaluation. *Information Sciences*, 191:192–213, 2012.
- 751 V C Bieker, F Sánchez Barreiro, J A Rasmussen, M Brunier, N Wales, and M D Martin. Metage-
752 nomic analysis of historical herbarium specimens reveals a postmortem microbial community.
753 *Molecular Ecology Resources*, 20(5):1206–1219, 2020.
- 754 J L Blois, P L Zarnetske, M C Fitzpatrick, and S Finnegan. Climate change and the past, present,
755 and future of biotic interactions. *Science*, 341(6145):499–504, 2013.
- 756 M Bradshaw, U Braun, M Elliott, J Kruse, S-Y Liu, G Guan, and P Tobin. A global genetic analysis
757 of herbarium specimens reveals the invasion dynamics of an introduced plant pathogen. *Fungal
758 Biology*, 125(8):585–595, 2021.

- 759 Michael J Bradshaw, Julie Carey, Miao Liu, Holly P Bartholomew, Wayne M Jurick, Sarah Hambleton, Dylan Hendricks, Martin Schnittler, and Markus Scholler. Genetic time traveling: sequencing old herbarium specimens, including the oldest herbarium specimen sequenced from kingdom fungi, reveals the population structure of an agriculturally significant rust. *New Phytologist*, 237(4):1463–1473, 2023.
- 764 D Brem and A Leuchtmann. *Epichloë* grass endophytes increase herbivore resistance in the woodland grass *Brachypodium sylvaticum*. *Oecologia*, 126(4):522–530, 2001.
- 766 DOMINIK Brem and ADRIAN Leuchtmann. High prevalence of horizontal transmission of the fungal endophyte epichloë sylvatica. *Bull. Geobot. Inst. ETH*, 65(3):12, 1999.
- 768 Stuart D Card, Marty J Faville, Wayne R Simpson, Richard D Johnson, Christine R Voisey, Anouck CM de Bonth, and David E Hume. Mutualistic fungal endophytes in the triticeae—survey and description. *FEMS Microbiology Ecology*, 88(1):94–106, 2014.
- 771 S Cheng, Y-N Zou, K Kuča, A Hashem, E F Abd_Allah, and Q-S Wu. Elucidating the mechanisms underlying enhanced drought tolerance in plants mediated by arbuscular mycorrhizal fungi. *Frontiers in Microbiology*, 12:4029, 2021.
- 774 K Clay and C Schardl. Evolutionary origins and ecological consequences of endophyte symbiosis with grasses. *The American Naturalist*, 160(S4):S99–S127, 2002.
- 776 D G Clayton, L Bernardinelli, and C Montomoli. Spatial correlation in ecological analysis. *International Journal of Epidemiology*, 22(6):1193–1202, 1993.
- 778 S D Côté, T P Rooney, J-P Tremblay, C Dussault, and D M Waller. Ecological impacts of deer overabundance. *Annu. Rev. Ecol. Evol. Syst.*, 35(1):113–147, 2004.
- 780 KD Craven, PTW Hsiau, A Leuchtmann, W Hollin, and CL Schardl. Multigene phylogeny of *Epichloë* species, fungal symbionts of grasses. *Annals of the Missouri Botanical Garden*, pages 14–34, 2001.

- 783 K M Crawford, J M Land, and J A Rudgers. Fungal endophytes of native grasses decrease insect
784 herbivore preference and performance. *Oecologia*, 164:431–444, 2010.
- 785 M S Crossley, T D Meehan, M D Moran, J Glassberg, W E Snyder, and A K Davis. Opposing
786 global change drivers counterbalance trends in breeding North American monarch butterflies.
787 *Global Change Biology*, 28(15):4726–4735, 2022.
- 788 C Daly and K Bryant. The PRISM climate and weather system — An introduction. *Corvallis, OR:*
789 *PRISM climate group*, 2, 2013.
- 790 B H Daru, D S Park, R B Primack, C G Willis, D S Barrington, T J S Whitfeld, T G Seidler, P W
791 Sweeney, D R Foster, A M Ellison, et al. Widespread sampling biases in herbaria revealed from
792 large-scale digitization. *New Phytologist*, 217(2):939–955, 2018.
- 793 B H Daru, E A Bowman, D H Pfister, and A E Arnold. A novel proof of concept for capturing
794 the diversity of endophytic fungi preserved in herbarium specimens. *Philosophical Transactions
795 of the Royal Society B*, 374(1763):20170395, 2019.
- 796 C C Davis, C G Willis, B Connolly, C Kelly, and A M Ellison. Herbarium records are reliable sources
797 of phenological change driven by climate and provide novel insights into species' phenological
798 cueing mechanisms. *American Journal of Botany*, 102(10):1599–1609, 2015.
- 799 Charles C Davis. The herbarium of the future. *Trends in Ecology & Evolution*, 38(5):412–423, 2023.
- 800 A J Davitt, M Stansberry, and H A Rudgers. Do the costs and benefits of fungal endophyte symbiosis
801 vary with light availability? *New Phytologist*, 188(3):824–834, 2010.
- 802 A J Davitt, C Chen, and J A Rudgers. Understanding context-dependency in plant–microbe sym-
803 biosis: The influence of abiotic and biotic contexts on host fitness and the rate of symbiont
804 transmission. *Environmental and Experimental Botany*, 71(2):137–145, 2011.
- 805 F A Decunta, L I Pérez, D P Malinowski, M A Molina-Montenegro, and P E Gundel. A systematic

- 806 review on the effects of *Epichloë* fungal endophytes on drought tolerance in cool-season grasses.
807 *Frontiers in Plant Science*, 12:644731, 2021.
- 808 M Di Luzio, G L Johnson, C Daly, J K Eischeid, and J G Arnold. Constructing retrospective
809 gridded daily precipitation and temperature datasets for the conterminous United States. *Journal*
810 *of Applied Meteorology and Climatology*, 47(2):475–497, 2008.
- 811 M L Donald, T F Bohner, K M Kolis, R A Shadow, J A Rudgers, and TEX Miller. Context-
812 dependent variability in the population prevalence and individual fitness effects of plant–fungal
813 symbiosis. *Journal of Ecology*, 109(2):847–859, 2021.
- 814 AE Douglas. Host benefit and the evolution of specialization in symbiosis. *Heredity*, 81(6):599–603,
815 1998.
- 816 Y-W Duan, H Ren, T Li, L-L Wang, Z-Q Zhang, Y-L Tu, and Y-P Yang. A century of pollination
817 success revealed by herbarium specimens of seed pods. *New Phytologist*, 224(4):1512–1517, 2019.
- 818 E J Edwards, B D Mishler, and C D Davis. University herbaria are uniquely important. *Trends in*
819 *Plant Science*.
- 820 M Engel, T Mette, and W Falk. Spatial species distribution models: Using Bayes inference with
821 INLA and SPDE to improve the tree species choice for important European tree species. *Forest*
822 *Ecology and Management*, 507:119983, 2022.
- 823 K D Erickson and A B Smith. Accounting for imperfect detection in data from museums and herbaria
824 when modeling species distributions: combining and contrasting data-level versus model-level bias
825 correction. *Ecography*, 44(9):1341–1352, 2021.
- 826 S M Evers, T M Knight, D W Inouye, TEX Miller, R Salguero-Gómez, A M Iler, and A Compagnoni.
827 Lagged and dormant season climate better predict plant vital rates than climate during the
828 growing season. *Global Change Biology*, 27(9):1927–1941, 2021.

- 829 P E M Fine. Vectors and vertical transmission: an epidemiologic perspective. *Annals of the New*
830 *York Academy of Sciences*, 266(1):173–194, 1975.
- 831 J C Fowler, M L Donald, J L Bronstein, and TEX Miller. The geographic footprint of mutualism:
832 How mutualists influence species' range limits. *Ecological Monographs*, 93(1):e1558, 2023.
- 833 J C Fowler, S Ziegler, K D Whitney, J A Rudgers, and TEX Miller. Microbial symbionts buffer
834 hosts from the demographic costs of environmental stochasticity. *Ecology Letters*, 27(5):e14438,
835 2024.
- 836 PR Frade, F De Jongh, F Vermeulen, J Van Bleijswijk, and RPM Bak. Variation in symbiont
837 distribution between closely related coral species over large depth ranges. *Molecular Ecology*, 17
838 (2):691–703, 2008.
- 839 M E Frederickson. Mutualisms are not on the verge of breakdown. *Trends in Ecology & Evolution*,
840 32(10):727–734, 2017.
- 841 W Gaul, D Sadykova, H J White, L Leon-Sanchez, P Caplat, M C Emmerson, and J M Yearsley.
842 Data quantity is more important than its spatial bias for predictive species distribution modelling.
843 *PeerJ*, 8:e10411, 2020.
- 844 GBIF.Org. Occurrence download, 2025a. URL <https://www.gbif.org/occurrence/download/>
845 0018831-250127130748423.
- 846 GBIF.Org. Occurrence download, 2025b. URL <https://www.gbif.org/occurrence/download/>
847 0018850-250127130748423.
- 848 GBIF.Org. Occurrence download, 2025c. URL <https://www.gbif.org/occurrence/download/>
849 0018851-250127130748423.
- 850 A Gelman and J Hill. *Data analysis using regression and multilevel/hierarchical models*. Cambridge
851 University Press, 2006.

- 852 S E Gilman, M C Urban, J Tewksbury, G W Gilchrist, and R D Holt. A framework for community
853 interactions under climate change. *Trends in Ecology & Evolution*, 25(6):325–331, 2010.
- 854 G Granath, M Vicari, D R Bazely, J P Ball, A Puentes, and T Rakocevic. Variation in the abundance
855 of fungal endophytes in fescue grasses along altitudinal and grazing gradients. *Ecography*, 30(3):
856 422–430, 2007.
- 857 A Gross, C Petitcollin, C Dutech, B Ly, M Massot, J Faivre d'Arcier, L Dubois, G Saint-Jean, and
858 M-L Desprez-Loustau. Hidden invasion and niche contraction revealed by herbaria specimens
859 in the fungal complex causing oak powdery mildew in europe. *Biological Invasions*, 23:885–901,
860 2021.
- 861 P E Gundel, I Zabalgogeazcoa, and BRV De Aldana. Interaction between plant genotype and
862 the symbiosis with *Epichloë* fungal endophytes in seeds of red fescue (*Festuca rubra*). *Crop and*
863 *Pasture Science*, 62(11):1010–1016, 2011a.
- 864 P E Gundel, A C Ueno, C Casas, TEX Miller, L I Pérez, R Cuyeu, and M Omacini. Temporal
865 host–symbiont dynamics in community contexts: Impacts of host fitness and vertical transmission
866 efficiency on symbiosis prevalence. *Functional Ecology*, 38(12):2610–2622, 2024.
- 867 Pedro E Gundel, Lucas Alejandro Garibaldi, María A Martínez-Ghersa, and Claudio M Ghersa.
868 Neotyphodium endophyte transmission to lolium multiflorum seeds depends on the host plant
869 fitness. *Environmental and Experimental Botany*, 71(3):359–366, 2011b.
- 870 Pedro E Gundel, Prudence Sun, Nikki D Charlton, Carolyn A Young, Tom EX Miller, and Jen-
871 nifer A Rudgers. Simulated folivory increases vertical transmission of fungal endophytes that
872 deter herbivores and alter tolerance to herbivory in poa autumnalis. *Annals of Botany*, 125(6):
873 981–991, 2020.
- 874 Pedro Emilio Gundel, Jennifer A Rudgers, and Claudio Marco Ghersa. Incorporating the process
875 of vertical transmission into understanding of host–symbiont dynamics. *Oikos*, 120(8):1121–1128,
876 2011c.

- 877 E K Hart and K Bell. *prism: Download data from the Oregon prism project*, 2015. URL <https://github.com/ropensci/prism>. R package version 0.0.6.
- 879 J J Heberling and D J Burke. Utilizing herbarium specimens to quantify historical mycorrhizal
880 communities. *Applications in plant sciences*, 7(4):e01223, 2019.
- 881 R J Hijmans, S Phillips, J Leathwick, J Elith, and Robert J Hijmans. Package ‘dismo’. *Circles*, 9
882 (1):1–68, 2017.
- 883 J HilleRisLambers, M A Harsch, A K Ettinger, K R Ford, and E J Theobald. How will biotic
884 interactions influence climate change-induced range shifts? *Annals of the New York Academy of
885 Sciences*, 1297(1):112–125, 2013.
- 886 Leopoldo J Iannone, James F White Jr, Liliana M Giussani, Daniel Cabral, and María Victoria
887 Novas. Diversity and distribution of neotyphodium-infected grasses in argentina. *Mycological
888 Progress*, 10(1):9–19, 2011.
- 889 IPCC. Climate change 2021: The physical science basis, 2021. URL <https://www.ipcc.ch/report/ar6/wg1/>.
- 891 N J B Isaac, M A Jarzyna, P Keil, L I Dambly, P H Boersch-Supan, E Browning, S N Freeman,
892 N Golding, G Guillera-Arroita, P A Henrys, et al. Data integration for large-scale models of
893 species distributions. *Trends in Ecology & Evolution*, 35(1):56–67, 2020.
- 894 Gareth James, Daniela Witten, Trevor Hastie, Robert Tibshirani, et al. *An introduction to statistical
895 learning*, volume 112. Springer, 2013.
- 896 A Jiménez-Valverde. Insights into the area under the receiver operating characteristic curve (auc)
897 as a discrimination measure in species distribution modelling. *Global Ecology and Biogeography*,
898 21(4):498–507, 2012.
- 899 D Kahle and H Wickham. Package ‘ggmap’. *Retrieved September*, 5:2021, 2019.

- 900 M R Kazenel, C L Debban, L Ranelli, W Q Hendricks, Y A Chung, T H Pendergast IV, N D
901 Charlton, C A Young, and J A Rudgers. A mutualistic endophyte alters the niche dimensions of
902 its host plant. *AoB plants*, 7:plv005, 2015.
- 903 R A Knapp, G M Fellers, P M Kleeman, D AW Miller, V T Vredenburg, E B Rosenblum, and C J
904 Briggs. Large-scale recovery of an endangered amphibian despite ongoing exposure to multiple
905 stressors. *Proceedings of the National Academy of Sciences*, 113(42):11889–11894, 2016.
- 906 M V Kozlov, I V Sokolova, V Zverev, A A Egorov, M Y Goncharov, and E L Zvereva. Biases in
907 estimation of insect herbivory from herbarium specimens. *Scientific Reports*, 10(1):12298, 2020.
- 908 Marcus Lapeyrolerie and Carl Boettiger. Limits to ecological forecasting: Estimating uncertainty
909 for critical transitions with deep learning. *Methods in Ecology and Evolution*, 14(3):785–798, 2023.
- 910 B R Lee, E F Alecrim, T K Miller, J RK Forrest, J M Heberling, R B Primack, and R D Sargent.
911 Phenological mismatch between trees and wildflowers: Reconciling divergent findings in two recent
912 analyses. *Journal of Ecology*, 112(6):1184–1199, 2024.
- 913 J Lendemer, B Thiers, A K Monfils, J Zaspel, E R Ellwood, A Bentley, K LeVan, J Bates, D Jen-
914 nings, D Contreras, et al. The extended specimen network: A strategy to enhance us biodiversity
915 collections, promote research and education. *BioScience*, 70(1):23–30, 2020.
- 916 A Leuchtmann. Systematics, distribution, and host specificity of grass endophytes. *Natural toxins*,
917 1(3):150–162, 1992.
- 918 A Leuchtmann, C W Bacon, C L Schardl, J F White Jr, and M Tadych. Nomenclatural realignment
919 of *Neotyphodium* species with genus *Epichloë*. *Mycologia*, 106(2):202–215, 2014.
- 920 F Lindgren, H Rue, and J Lindström. An explicit link between gaussian fields and gaussian markov
921 random fields: the stochastic partial differential equation approach. *Journal of the Royal Statis-
922 tical Society: Series B (Statistical Methodology)*, 73(4):423–498, 2011.

- 923 C Liu, P M Berry, T P Dawson, and R G Pearson. Selecting thresholds of occurrence in the
924 prediction of species distributions. *Ecography*, 28(3):385–393, 2005.
- 925 D D Mc Cargo, L J Iannone, M V Vignale, C L Schardl, and M S Rossi. Species diversity of
926 *Epichloë* symbiotic with two grasses from southern Argentinean Patagonia. *Mycologia*, 106(2):
927 339–352, 2014.
- 928 M McFall-Ngai, M G Hadfield, TCG Bosch, H V Carey, T Domazet-Lošo, A E Douglas, N Dubilier,
929 G Eberl, T Fukami, S F Gilbert, et al. Animals in a bacterial world, a new imperative for the
930 life sciences. *Proceedings of the National Academy of Sciences*, 110(9):3229–3236, 2013.
- 931 T D Meehan, N L Michel, and H Rue. Spatial modeling of Audubon Christmas Bird Counts reveals
932 fine-scale patterns and drivers of relative abundance trends. *Ecosphere*, 10(4):e02707, 2019.
- 933 Gerrit Meijer and Adrian Leuchtmann. The effects of genetic and environmental factors on disease
934 expression (stroma formation) and plant growth in *brachypodium sylvaticum* infected by epichloë
935 *sylvatica*. *Oikos*, 91(3):446–458, 2000.
- 936 E K Meineke and B H Daru. Bias assessments to expand research harnessing biological collections.
937 *Trends in Ecology & Evolution*, 36(12):1071–1082, 2021.
- 938 E K Meineke, C C Davis, and T J Davies. The unrealized potential of herbaria for global change
939 biology. *Ecological Monographs*, 88(4):505–525, 2018.
- 940 E K Meineke, A T Classen, N J Sanders, and T J Davies. Herbarium specimens reveal increasing
941 herbivory over the past century. *Journal of Ecology*, 107(1):105–117, 2019.
- 942 A R Meyer, M Valentin, L Liulevicius, T R McDonald, M P Nelsen, J Pengra, R J Smith, and
943 D Stanton. Climate warming causes photobiont degradation and carbon starvation in a boreal climate
944 sentinel lichen. *American Journal of Botany*, 2022.
- 945 D AW Miller, K Pacifici, J S Sanderlin, and B J Reich. The recent past and promising future for

- 946 data integration methods to estimate species' distributions. *Methods in Ecology and Evolution*,
947 10(1):22–37, 2019.
- 948 D S Park, I Breckheimer, A C Williams, E Law, A M Ellison, and C C Davis. Herbarium specimens
949 reveal substantial and unexpected variation in phenological sensitivity across the eastern United
950 States. *Philosophical Transactions of the Royal Society B*, 374(1763):20170394, 2019.
- 951 B J Parker, J Hrček, AHC McLean, and H C J Godfray. Genotype specificity among hosts,
952 pathogens, and beneficial microbes influences the strength of symbiont-mediated protection. *Evo-*
953 *lution*, 71(5):1222–1231, 2017.
- 954 M Parniske. Arbuscular mycorrhiza: The mother of plant root endosymbioses. *Nature Reviews*
955 *Microbiology*, 6(10):763–775, 2008.
- 956 A Pauw and J A Hawkins. Reconstruction of historical pollination rates reveals linked declines of
957 pollinators and plants. *Oikos*, 120(3):344–349, 2011.
- 958 S Piao, Q Liu, A Chen, I A Janssens, Y Fu, J Dai, L Liu, X Lian, M Shen, and X Zhu. Plant
959 phenology and global climate change: Current progresses and challenges. *Global Change Biology*,
960 25(6):1922–1940, 2019.
- 961 T Poisot, G Bergeron, K Cazelles, T Dallas, D Gravel, A MacDonald, B Mercier, C Violet, and
962 S Vissault. Global knowledge gaps in species interaction networks data. *Journal of Biogeography*,
963 48(7):1552–1563, 2021.
- 964 N E Rafferty, P J CaraDonna, and J L Bronstein. Phenological shifts and the fate of mutualisms.
965 *Oikos*, 124(1):14–21, 2015.
- 966 Emma Chollet Ramampiandra, Andreas Scheidegger, Jonas Wydler, and Nele Schuwirth. A com-
967 parison of machine learning and statistical species distribution models: Quantifying overfitting
968 supports model interpretation. *Ecological Modelling*, 481:110353, 2023.

- 969 C J Raxworthy and B T Smith. Mining museums for historical DNA: Advances and challenges in
970 museomics. *Trends in Ecology & Evolution*, 36(11):1049–1060, 2021.
- 971 F Renoz, I Pons, and T Hance. Evolutionary responses of mutualistic insect–bacterial symbioses in
972 a world of fluctuating temperatures. *Current Opinion in Insect Science*, 35:20–26, 2019.
- 973 Jean B Ristaino. The importance of mycological and plant herbaria in tracking plant killers. *Fron-
974 tiers in Ecology and Evolution*, 7:521, 2020.
- 975 Jean B Ristaino, Carol T Groves, and Gregory R Parra. Pcr amplification of the irish potato famine
976 pathogen from historic specimens. *Nature*, 411(6838):695–697, 2001.
- 977 Jean Beagle Ristaino. Tracking historic migrations of the irish potato famine pathogen, phytoph-
978 thora infestans. *Microbes and infection*, 4(13):1369–1377, 2002.
- 979 E L Roberts and A Ferraro. Rhizosphere microbiome selection by *Epichloë* endophytes of *Festuca*
980 *arundinacea*. *Plant and Soil*, 396:229–239, 2015.
- 981 RJ Rodriguez, JF White Jr, Anne E Arnold, and a RS and Redman. Fungal endophytes: diversity
982 and functional roles. *New Phytologist*, 182(2):314–330, 2009.
- 983 G Rolshausen, F Dal Grande, A D Sadowska-Deś, J Otte, and I Schmitt. Quantifying the climatic
984 niche of symbiont partners in a lichen symbiosis indicates mutualist-mediated niche expansions.
985 *Ecography*, 41(8):1380–1392, 2018.
- 986 J A Rudgers, M E Afkhami, M A Rúa, A J Davitt, S Hammer, and V M Huguet. A fungus among
987 us: broad patterns of endophyte distribution in the grasses. *Ecology*, 90(6):1531–1539, 2009.
- 988 J A Rudgers, M E Afkhami, L Bell-Dereske, Y A Chung, K M Crawford, S N Kivlin, M A Mann,
989 and M A Nuñez. Climate disruption of plant-microbe interactions. *Annual review of ecology,
990 evolution, and systematics*, 51(1):561–586, 2020.
- 991 Jennifer A Rudgers and Angela L Swafford. Benefits of a fungal endophyte in *Elymus virginicus*
992 decline under drought stress. *Basic and Applied Ecology*, 10(1):43–51, 2009.

- 993 H Rue, S Martino, and N Chopin. Approximate bayesian inference for latent gaussian models by
994 using integrated nested laplace approximations. *Journal of the royal statistical society: Series b*
995 (*statistical methodology*), 71(2):319–392, 2009.
- 996 R F Sage. Global change biology: a primer. *Global Change Biology*, 26(1):3–30, 2020.
- 997 K Saikkonen, P E Gundel, and M Helander. Chemical ecology mediated by fungal endophytes in
998 grasses. *Journal of chemical ecology*, 39:962–968, 2013.
- 999 C L Schardl, C A Young, J R Faulkner, S Florea, and J Pan. Chemotypic diversity of *Epichloae*,
1000 fungal symbionts of grasses. *Fungal Ecology*, 5(3):331–344, 2012.
- 1001 Ryan J Schmidt, Kristen E Saban, Lena Struwe, and Charles C Davis. The collector practices that
1002 shape spatial, temporal, and taxonomic bias in herbaria. *New Phytologist*.
- 1003 María Semmartin, Marina Omacini, Pedro E Gundel, and Ignacio M Hernández-Agramonte. Broad-
1004 scale variation of fungal-endophyte incidence in temperate grasses. *Journal of Ecology*, 103(1):
1005 184–190, 2015.
- 1006 S I Seneviratne, X Zhang, M Adnan, W Badi, C Dereczynski, A D Luca, S Ghosh, I Iskandar,
1007 J Kossin, S Lewis, et al. Weather and climate extreme events in a changing climate. 2021.
- 1008 D Simpson, H Rue, A Riebler, T G Martins, and S H Sørbye. Penalising model component com-
1009 plexity: A principled, practical approach to constructing priors. 2017.
- 1010 Brajesh K Singh, Manuel Delgado-Baquerizo, Eleonora Egidi, Emilio Guirado, Jan E Leach, Hong-
1011 wei Liu, and Pankaj Trivedi. Climate change impacts on plant pathogens, food security and paths
1012 forward. *Nature Reviews Microbiology*, 21(10):640–656, 2023.
- 1013 Michelle E Sneck, Jennifer A Rudgers, Carolyn A Young, and Tom EX Miller. Variation in the
1014 prevalence and transmission of heritable symbionts across host populations in heterogeneous en-
1015 vironments. *Microbial Ecology*, 74:640–653, 2017.

- 1016 Pamela S Soltis. Digitization of herbaria enables novel research. *American journal of botany*, 104
1017 (9):1281–1284, 2017.
- 1018 T F Stocker, D Qin, G-K Plattner, L V Alexander, S K Allen, N L Bindoff, F-M Bréon, J A Church,
1019 U Cubasch, S Emori, et al. Technical summary. In *Climate Change 2013: The Physical Science
1020 Basis. Contribution of Working Group I to the Fifth Assessment Report of the Intergovernmental
1021 Panel on Climate Change*, pages 33–115. Cambridge University Press, 2013.
- 1022 S Sully, DE Burkepile, MK Donovan, G Hodgson, and R Van Woesik. A global analysis of coral
1023 bleaching over the past two decades. *Nature communications*, 10(1):1–5, 2019.
- 1024 Mariusz Tadych, Marshall S Bergen, and James F White Jr. Epichloë spp. associated with grasses:
1025 new insights on life cycles, dissemination and evolution. *Mycologia*, 106(2):181–201, 2014.
- 1026 Zipeng Tian, Ruying Wang, Karen V Ambrose, Bruce B Clarke, and Faith C Belanger. The epichloë
1027 festucae antifungal protein has activity against the plant pathogen sclerotinia homoeocarpa, the
1028 causal agent of dollar spot disease. *Scientific reports*, 7(1):5643, 2017.
- 1029 Tammy Tintjer, Adrian Leuchtmann, and Keith Clay. Variation in horizontal and vertical trans-
1030 mission of the endophyte epichloë elymi infecting the grass elymus hystrix. *New Phytologist*, 179
1031 (1):236–246, 2008.
- 1032 E Toby Kiers, T M Palmer, A R Ives, J F Bruno, and J L Bronstein. Mutualisms in a changing
1033 world: an evolutionary perspective. *Ecology Letters*, 13(12):1459–1474, 2010.
- 1034 A T Tredennick, G Hooker, S P Ellner, and P B Adler. A practical guide to selecting models for
1035 exploration, inference, and prediction in ecology. *Ecology*, 102(6):e03336, 2021.
- 1036 A D Treindl, J Stapley, and A Leuchtmann. Genetic diversity and population structure of *Epichloë*
1037 fungal pathogens of plants in natural ecosystems. *Frontiers in Ecology and Evolution*, 11:1129867,
1038 2023.

- 1039 A M Truitt, M Kapun, R Kaur, and W J Miller. Wolbachia modifies thermal preference in drosophila
1040 melanogaster. *Environmental microbiology*, 21(9):3259–3268, 2019.
- 1041 Shripad D. Tuljapurkar. Population dynamics in variable environments. III. Evolutionary dynamics
1042 of r-selection. *Theoretical Population Biology*, 21(1):141–165, February 1982. ISSN 0040-5809.
1043 doi: 10.1016/0040-5809(82)90010-7. URL <http://www.sciencedirect.com/science/article/pii/0040580982900107>.
- 1045 A Urdangarin, T Goicoa, and M D Ugarte. Evaluating recent methods to overcome spatial con-
1046 founding. *Revista Matemática Complutense*, 36(2):333–360, 2023.
- 1047 V Vikuk, C A Young, S T Lee, P Nagabhyru, M Krischke, M J Mueller, and J Krauss. Infection
1048 rates and alkaloid patterns of different grass species with systemic *Epichloë* endophytes. *Applied*
1049 *and Environmental Microbiology*, 85(17):e00465–19, 2019.
- 1050 M von Cräutlein, M Helander, H Korpelainen, P H Leinonen, B R Vázquez de Aldana, C A Young,
1051 I Zabalgogeazcoa, and K Saikkonen. Genetic diversity of the symbiotic fungus *Epichloë festucae*
1052 in naturally occurring host grass populations. *Frontiers in Microbiology*, 12:756991, 2021.
- 1053 Z Wang, C Li, and J White. Effects of *Epichloë* endophyte infection on growth, physiological
1054 properties and seed germination of wild barley under saline conditions. *Journal of Agronomy and*
1055 *Crop Science*, 206(1):43–51, 2020.
- 1056 Eric J Ward, Eli E Holmes, James T Thorson, and Ben Collen. Complexity is costly: a meta-
1057 analysis of parametric and non-parametric methods for short-term population forecasting. *Oikos*,
1058 123(6):652–661, 2014.
- 1059 R J Warren and M A Bradford. Mutualism fails when climate response differs between interacting
1060 species. *Global Change Biology*, 20(2):466–474, 2014.
- 1061 N S Webster, R E Cobb, and A P Negri. Temperature thresholds for bacterial symbiosis with a
1062 sponge. *The ISME journal*, 2(8):830–842, 2008.

- 1063 J F White and G T Cole. Endophyte-host associations in forage grasses. i. Distribution of fungal
1064 endophytes in some species of *Lolium* and *Festuca*. *Mycologia*, 77(2):323–327, 1985.
- 1065 F M Willems, JF Scheepens, and O Bosdorf. Forest wildflowers bloom earlier as europe warms:
1066 Lessons from herbaria and spatial modelling. *New Phytologist*, 235(1):52–65, 2022.
- 1067 C G Willis, E R Ellwood, R B Primack, C C Davis, K D Pearson, A S Gallinat, J M Yost, G Nelson,
1068 S J Mazer, N L Rossington, et al. Old plants, new tricks: Phenological research using herbarium
1069 specimens. *Trends in Ecology & Evolution*, 32(7):531–546, 2017.
- 1070 C Xia, N Li, Y Zhang, C Li, X Zhang, and Z Nan. Role of *Epichloë* endophytes in defense responses
1071 of cool-season grasses to pathogens: A review. *Plant Disease*, 102(11):2061–2073, 2018.
- 1072 K Yoshida, E Sasaki, and S Kamoun. Computational analyses of ancient pathogen DNA from
1073 herbarium samples: Challenges and prospects. *Frontiers in Plant Science*, 6:771, 2015.
- 1074 Kentaro Yoshida, Verena J Schuenemann, Liliana M Cano, Marina Pais, Bagdevi Mishra, Rahul
1075 Sharma, Chirsta Lanz, Frank N Martin, Sophien Kamoun, Johannes Krause, et al. The rise and
1076 fall of the *phytophthora infestans* lineage that triggered the irish potato famine. *elife*, 2:e00731,
1077 2013.

1078

Appendix A

1079

1080 *Appendix to "Increasing Prevalence of plant-fungal symbiosis across two*
1081 *centuries of environmental change"*

1082 **Authors:**

1083 Joshua C. Fowler^{1,2*}

1084 Jacob Moutouama¹

1085 Tom E. X. Miller¹

1086

1087 1. Rice University, Department of BioSciences, Houston, Texas 77006

1088 2. University of Miami, Department of Biology, Miami, Florida

1089 * Corresponding author; e-mail: jcf221@miami.edu.

1090 **Contents:**

1091 Appendix A includes: Figure A1 - Figure A15, Table A1, and Supporting Methods).

1092

Supplemental Figures

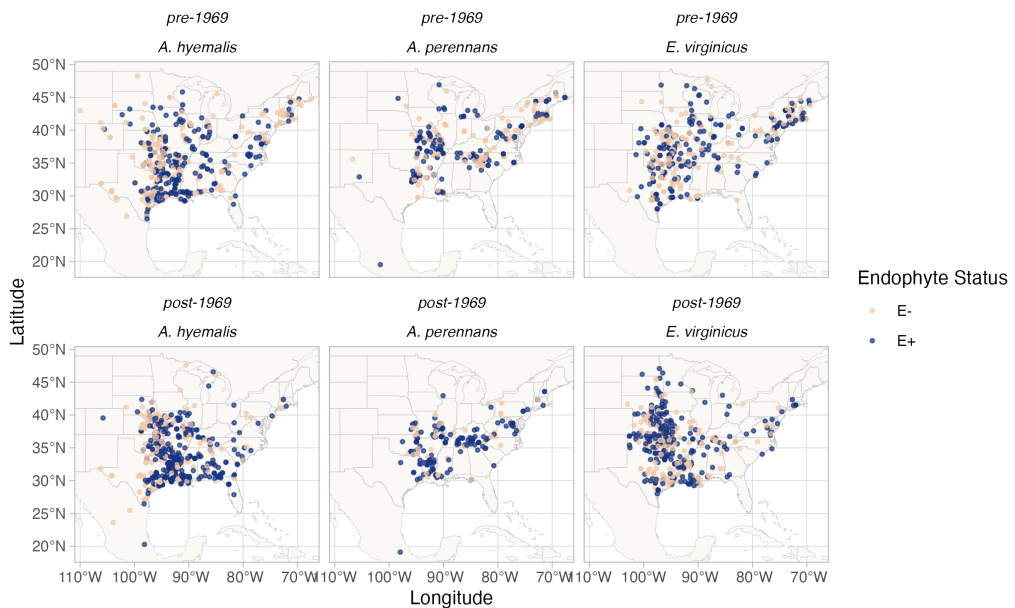


Figure A1: Endophyte presence/absence in specimens of each host species. Points show collection locations colored according to whether the specimen contained endophytes (E+; blue points) or did not contain endophytes (E-, tan points). To visualize temporal change, the data are faceted before and after the median year of collection. Map lines delineate study areas and do not necessarily depict accepted national boundaries.

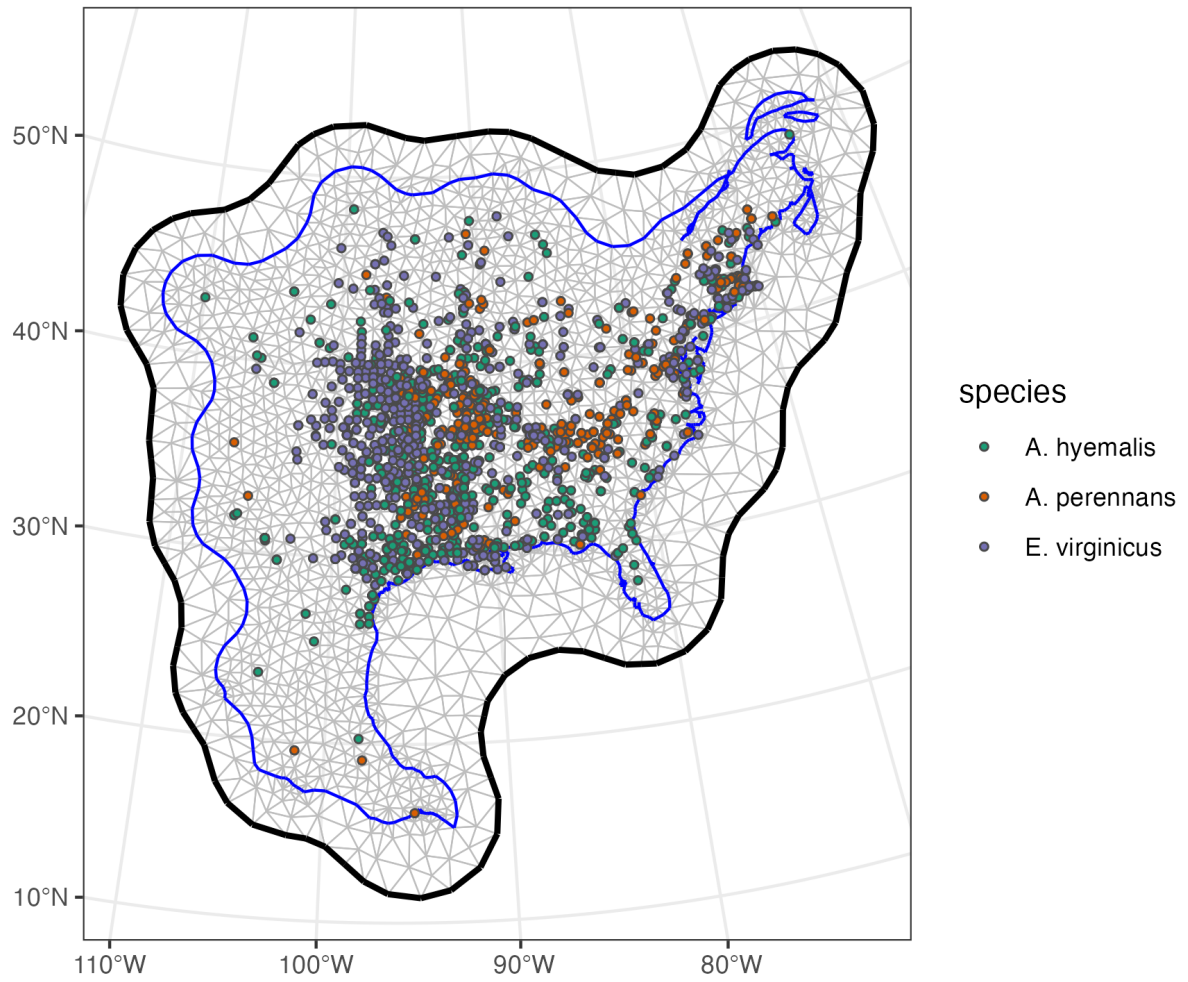


Figure A2: Triangulation mesh used to estimate spatial dependence between data points.

Grey lines indicate edges of triangles used to define distances between observations. Colored points indicate locations of sampled herbarium specimens for each host species, and the blue line shows the convex hull and coastline used to define the edge of the mesh around the data points. The thick black line shows the convex hull defining a buffer space around the edge of the mesh to reduce the influence of edge effects on model estimates.

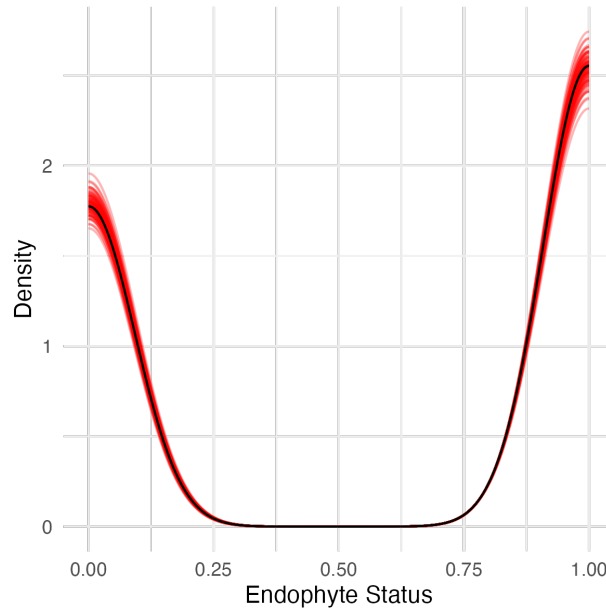


Figure A3: **Graphical posterior predictive check of the endophyte prevalence model fit.**

Consistency between observed data and predicted values indicate that the fitted model accurately describes the data. Graph shows density curves for the observed data (black) along with 100 predicted datasets (red).

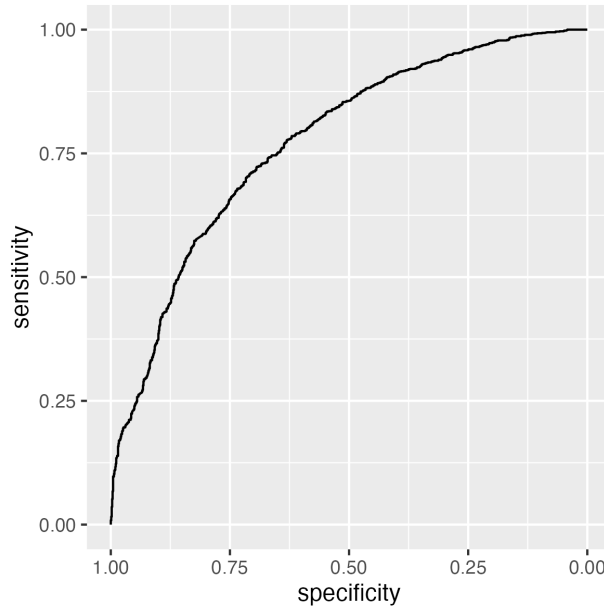


Figure A4: ROC plot showing performance of the endophyte prevalence model in classifying observations according to endophyte status within the in-sample training data from herbarium collections. The curves show adequate model performance for observed data. The AUC value is 0.79.

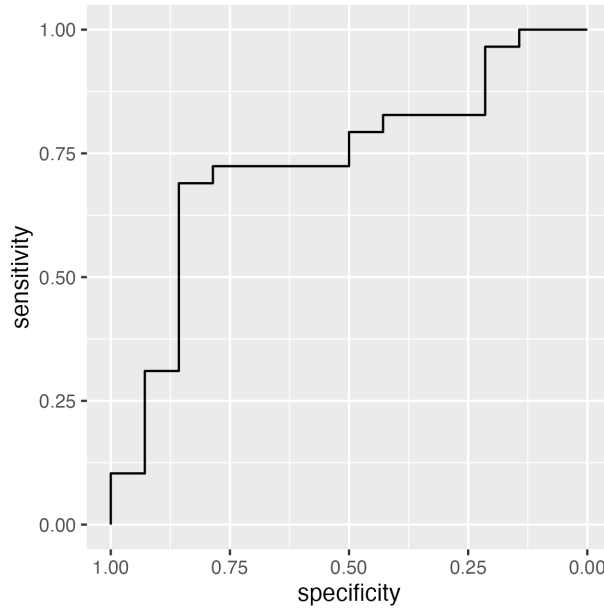


Figure A5: ROC plot showing performance of the endophyte prevalence model in classifying observations according to endophyte status within the out-of-sample test data from contemporary surveys. The curves show adequate model performance for test data. The AUC value is 0.77.

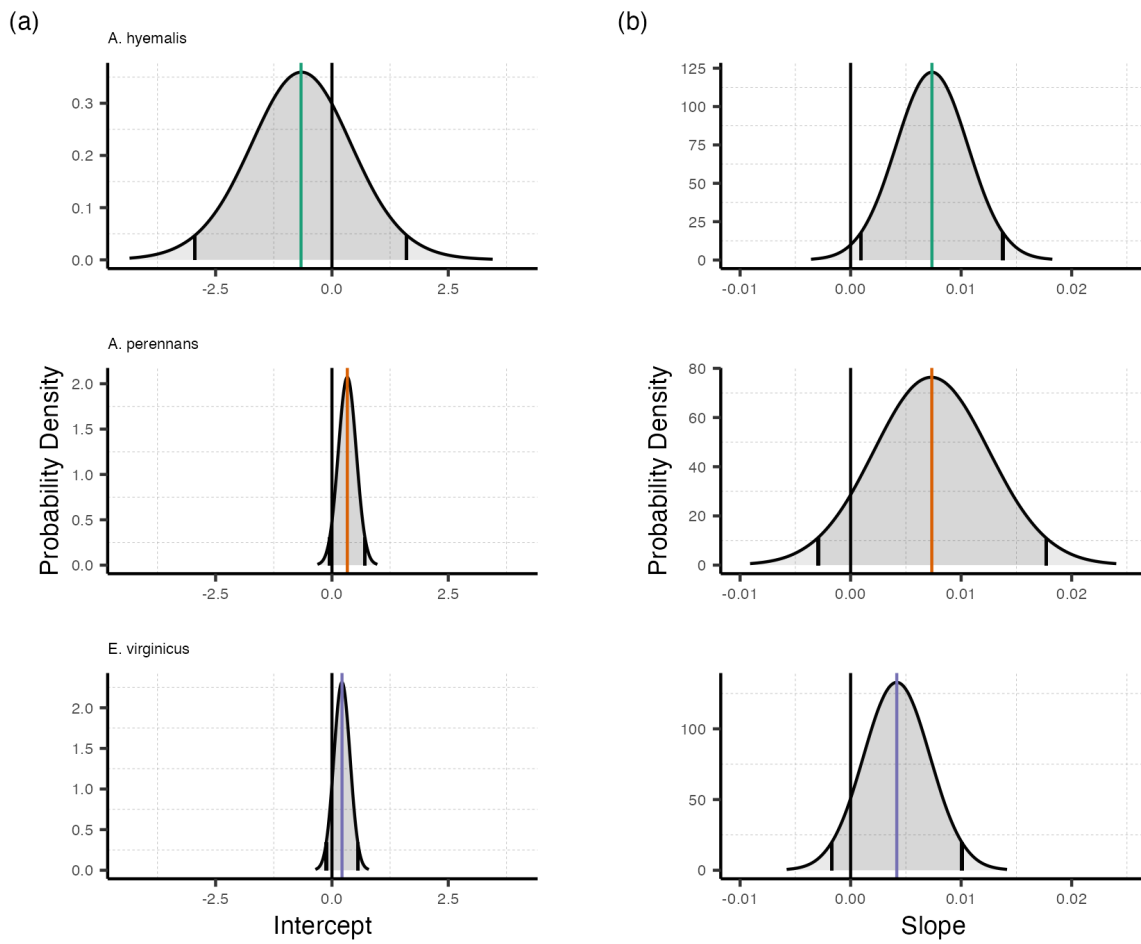


Figure A6: Posterior estimates of parameters describing global intercept and temporal trends from the endophyte prevalence model. Density curves show the probability density along with mean (colored line) and 95% CI (black lines) for the (A) intercept and (B) slope terms, A and T respectively from Eqn. 1. Colors represent each host species

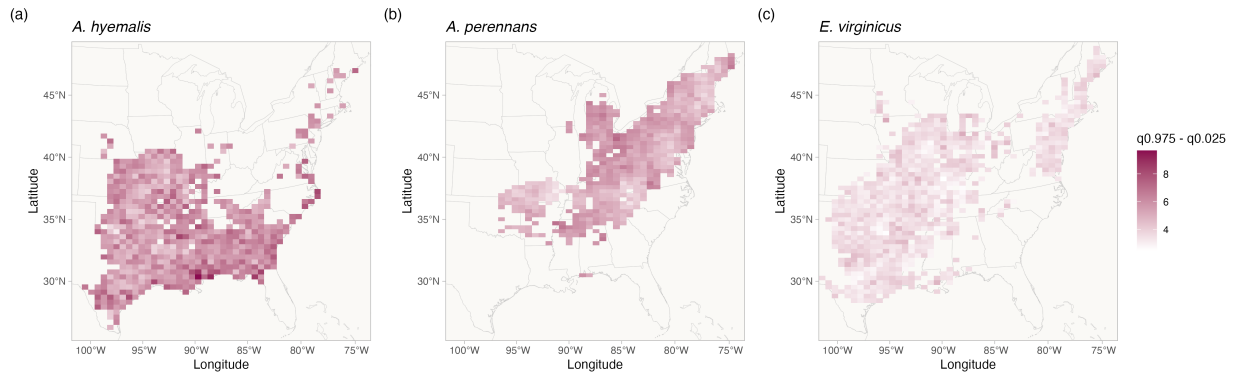


Figure A7: Credible interval width of temporal trends in endophyte prevalence across the distribution of each host species estimated from the endophyte prevalence model.
 Shading represents the range of the 95% posterior credible interval given in units of $\%$ *change in prevalence/year* for spatially varying slopes, τ from Eqn. 1. Map lines delineate study areas and do not necessarily depict accepted national boundaries.

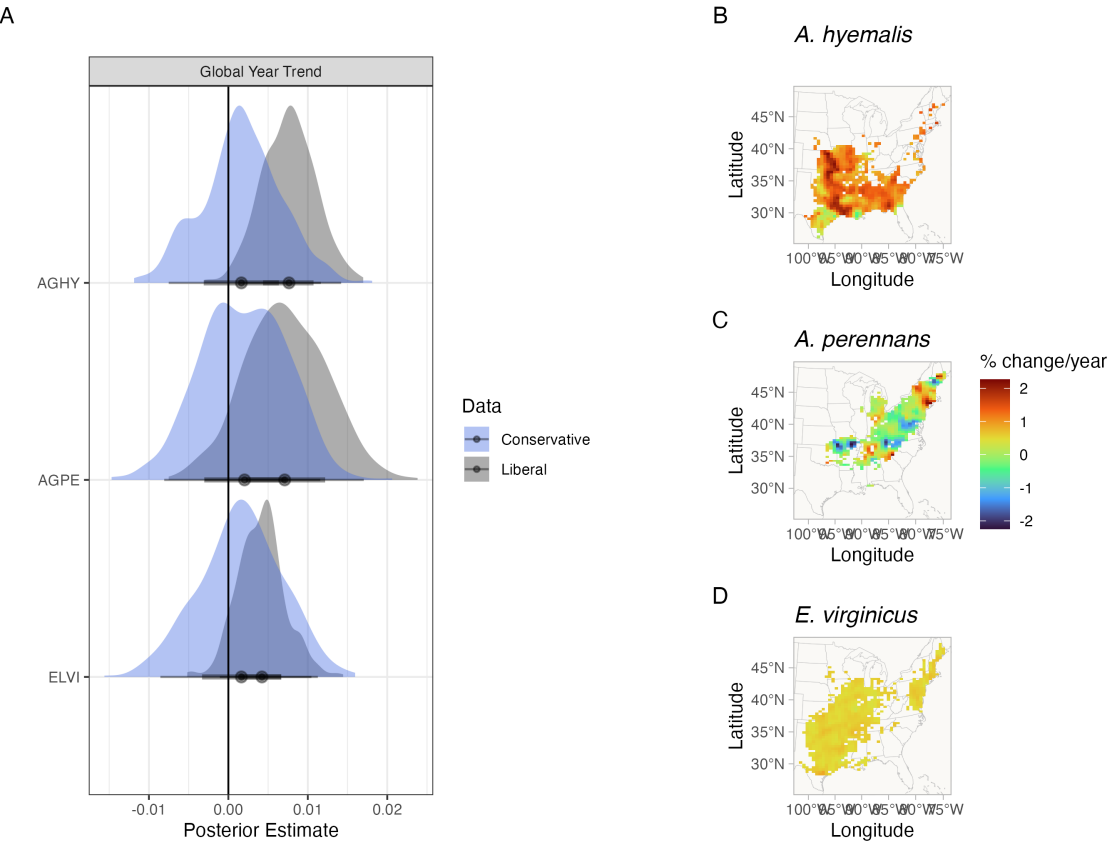


Figure A8: Comparison of endophyte prevalence model estimates fit to data with liberal versus conservative endophyte scores. Liberal and conservative scores document uncertainty in the endophyte identification process. Each specimen was given both a liberal and conservative scores. In cases of uncertain identification, the liberal status assumed a potential endophyte identification was more likely to be endophyte-positive while the conservative status assumed that the potential endophyte identification was less likely to be endophyte-positive. (A) Posterior estimates of global temporal trend (T from Eqn. 1) for the endophyte prevalence model fit to liberal scores (grey) and to conservative scores (blue). Maps show the spatially varying temporal trend estimates (τ from Eqn. 1) from the endophyte prevalence model fit to conservative scores for (B) *A. hyemalis*, (C) *A. perennans*, and (D) *E. virginicus*. Note that the color scale differs between this visualization and Fig. 3 that shows estimates fit using liberal endophyte scores.

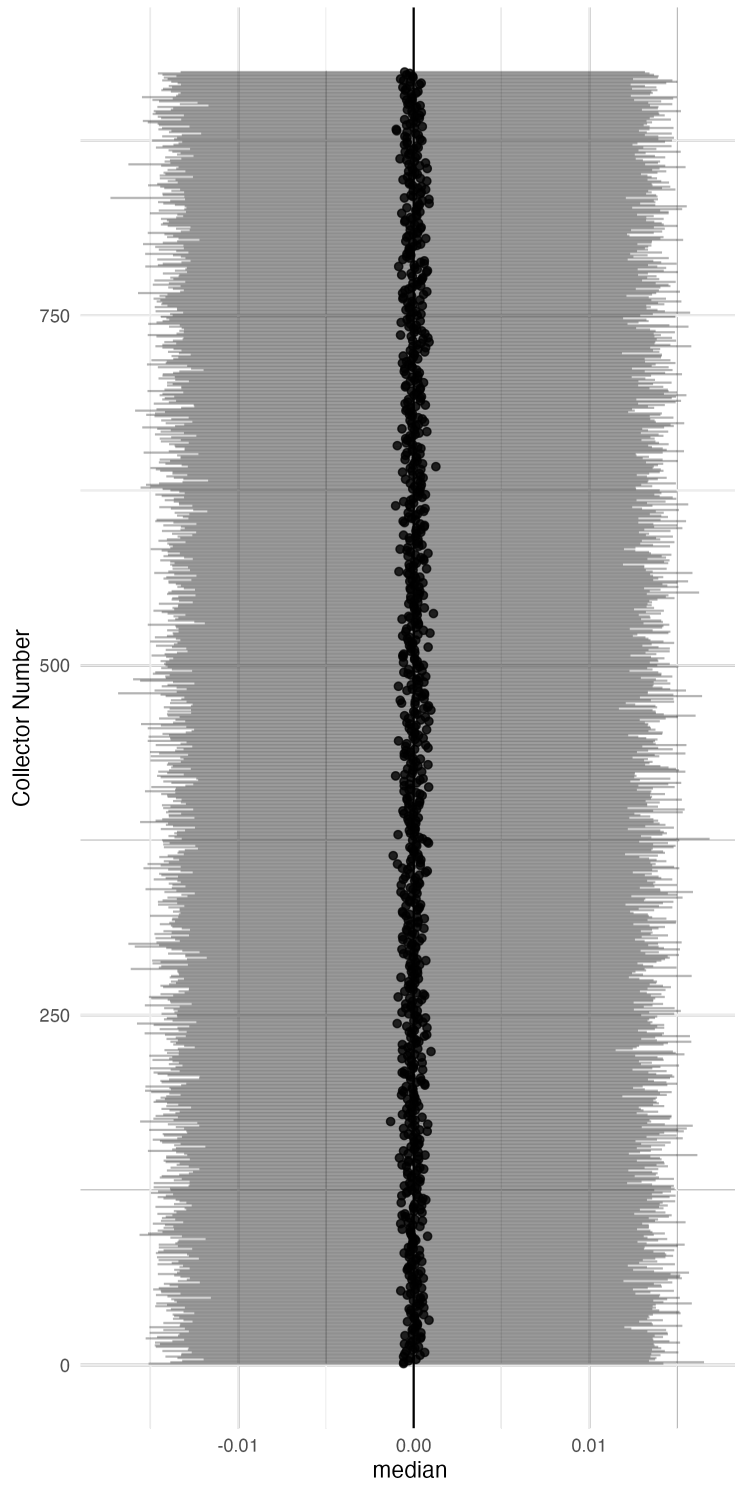


Figure A9: **Posterior estimates of collector random effects from endophyte prevalence model.** Collector random effects are denoted χ in Eqn. 1 and represent variance associated with researchers who collected historic herbarium specimens. Points show posterior median along with 95% CI for each of 924 individual collectors.

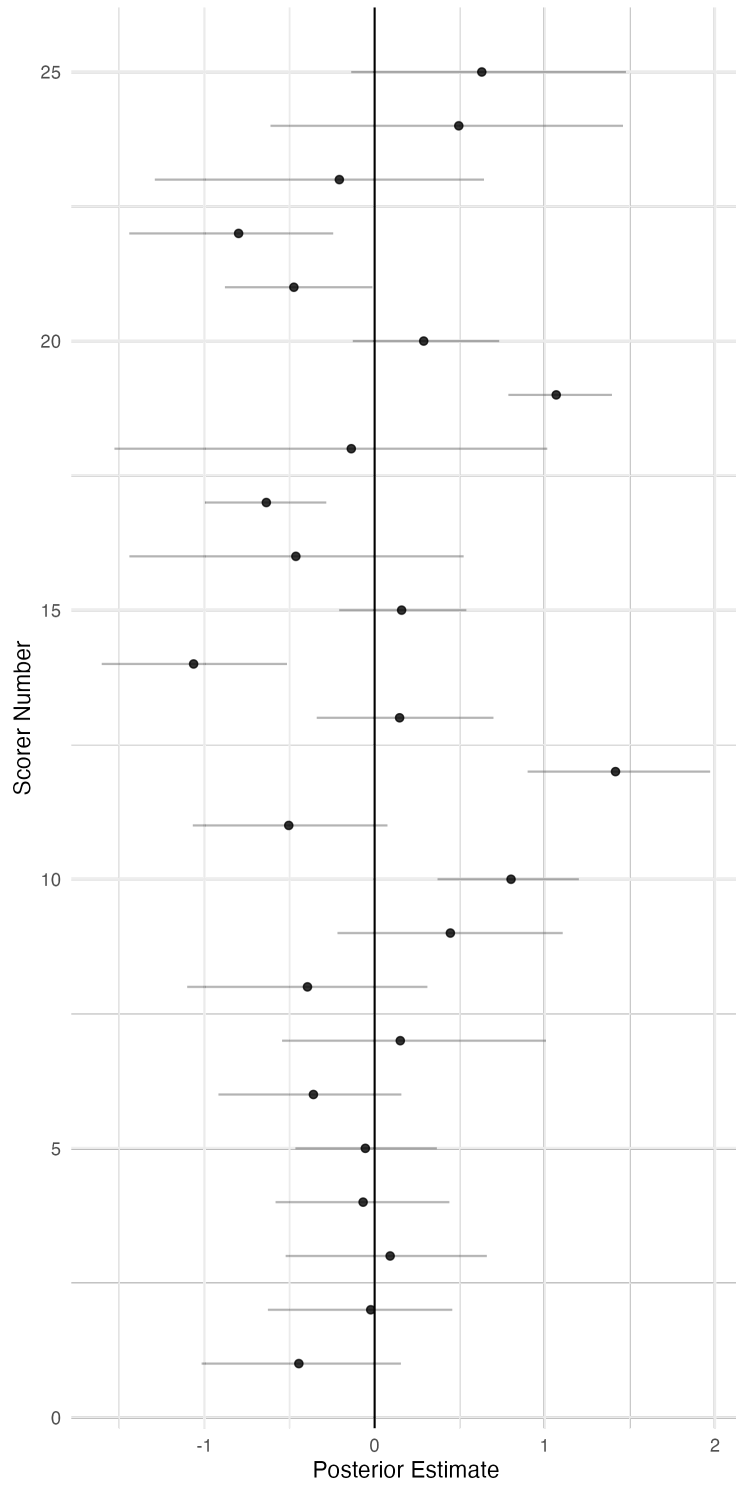


Figure A10: Posterior estimates of scorer random effects from endophyte prevalence model. Scorer random effects are denoted ω in Eqn. 1 and represent variance associated with researchers who identified *Epichloë* endophytes within herbarium specimen tissue samples. Points show posterior median along with 95% CI for each of 25 individual scorers.

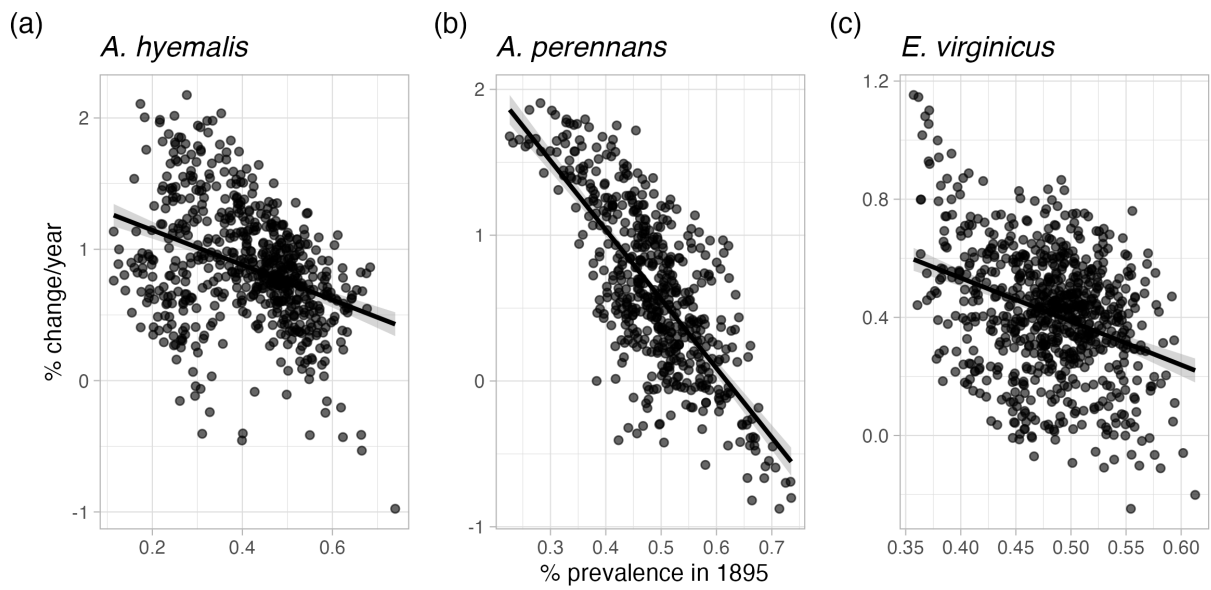


Figure A11: Relationship between initial prevalence and temporal trends in prevalence estimated from the endophyte prevalence model. Points show predicted posterior mean temporal trend for each species at pixels across each host distribution ((A) *A. hyemalis*, (B) *A. perennans*, and (C) *E. virginicus*). along with a linear regression and shaded ribbon showing 95% confidence interval.

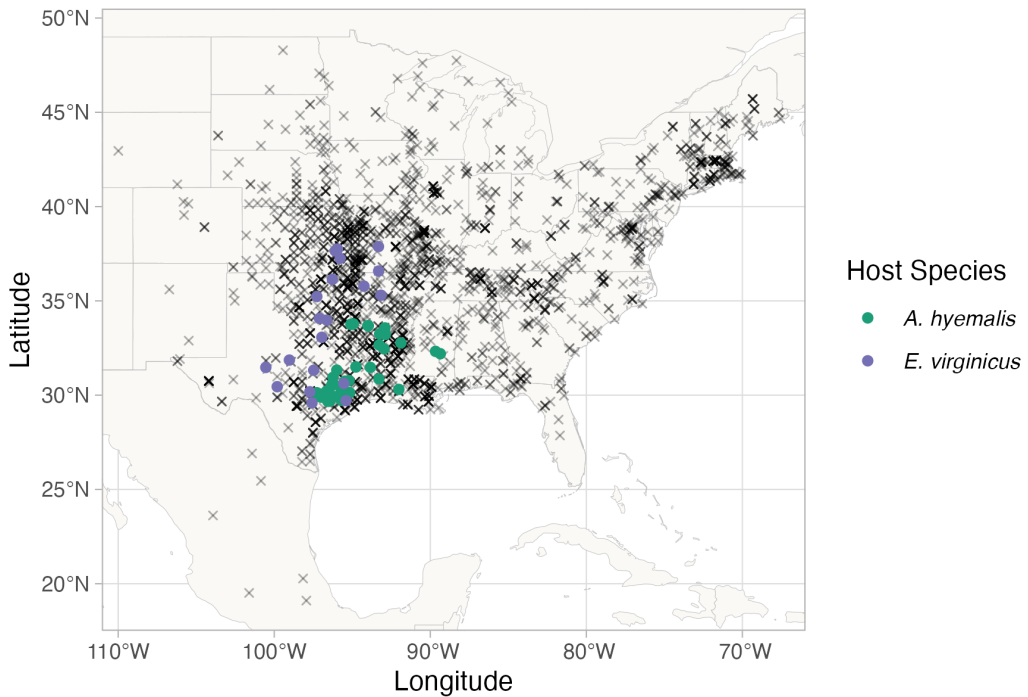
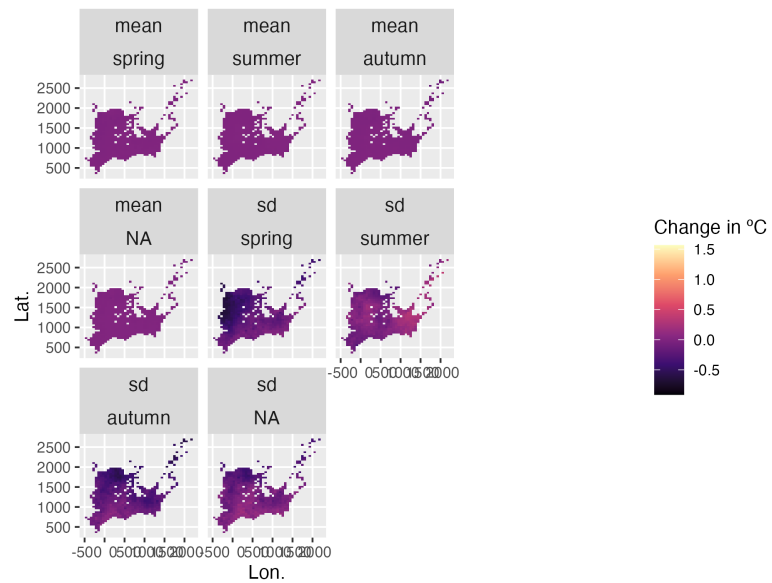


Figure A12: Locations of contemporary surveys of endophytes used as "test" data to evaluate predictive ability of the endophyte prevalence model. Points are locations of host populations surveyed between 2013 and 2019 for endophytes, colored by species (*A. hyemalis*: green, *E. virginicus*: purple). Black crosses show the historical herbarium collection locations used as "training" data for the endophyte prevalence model.

(a)



(b)

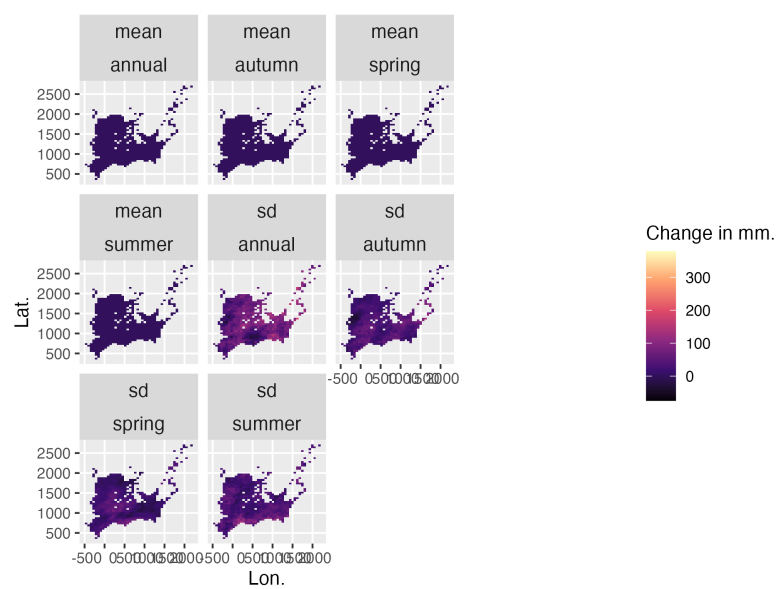
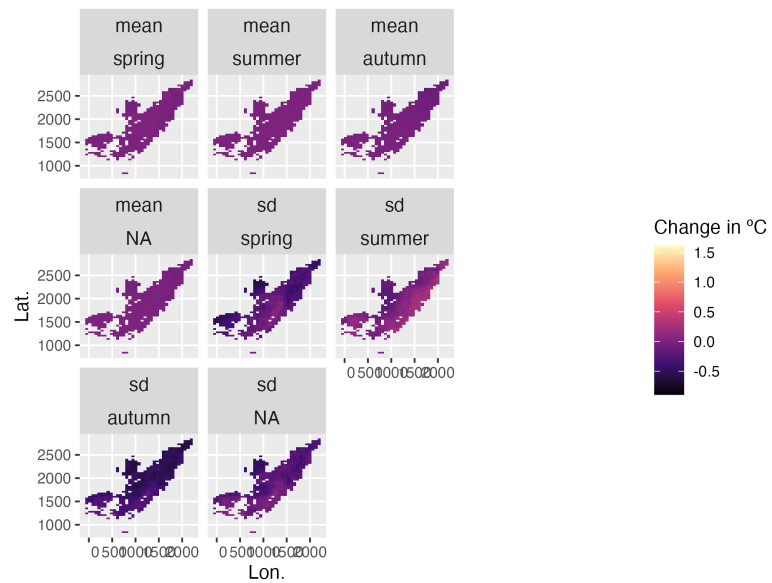


Figure A13: **Change in seasonal climate variables between the periods 1895-1925 and 1990-2020 across the distribution of *A. hyemalis*.** Color represents change in (A) seasonal temperature (°C) and (B) seasonal precipitation (mm.). Maps show pixels covering the modeled distribution of *A. hyemalis* used in *post hoc* climate regression analysis.

(a)



(b)

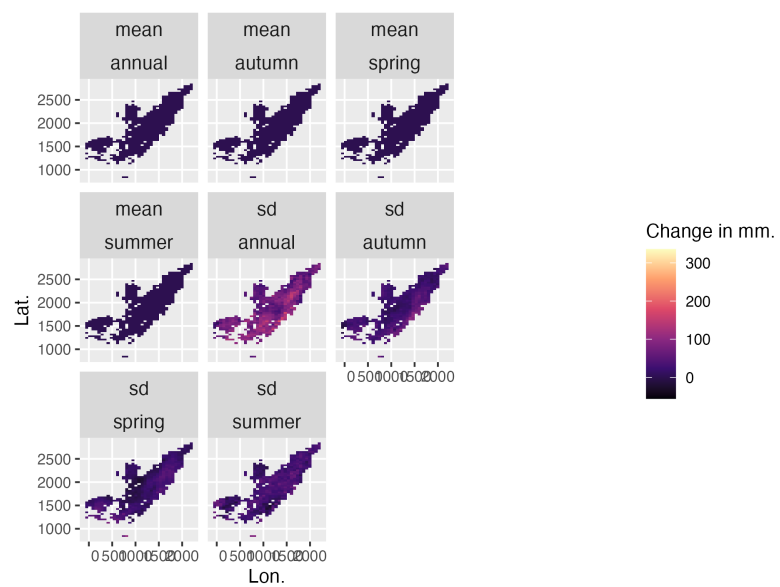
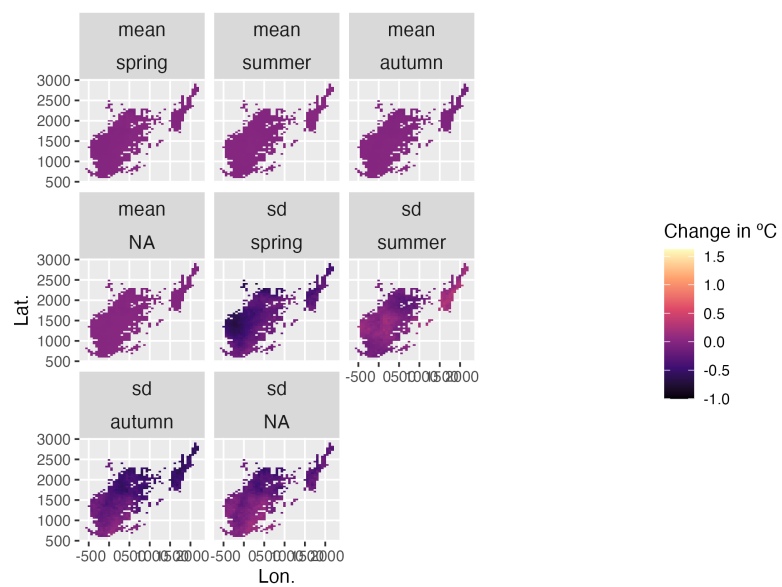


Figure A14: Change in seasonal climate variables between the periods 1895-1925 and 1990-2020 across the distribution of *A. perennans*. Color represents change in (A) seasonal temperature ($^{\circ}\text{C}$) and (B) seasonal precipitation (mm.). Maps show pixels covering the modeled distribution of *A. perennans* used in *post hoc* climate regression analysis.

(a)



(b)

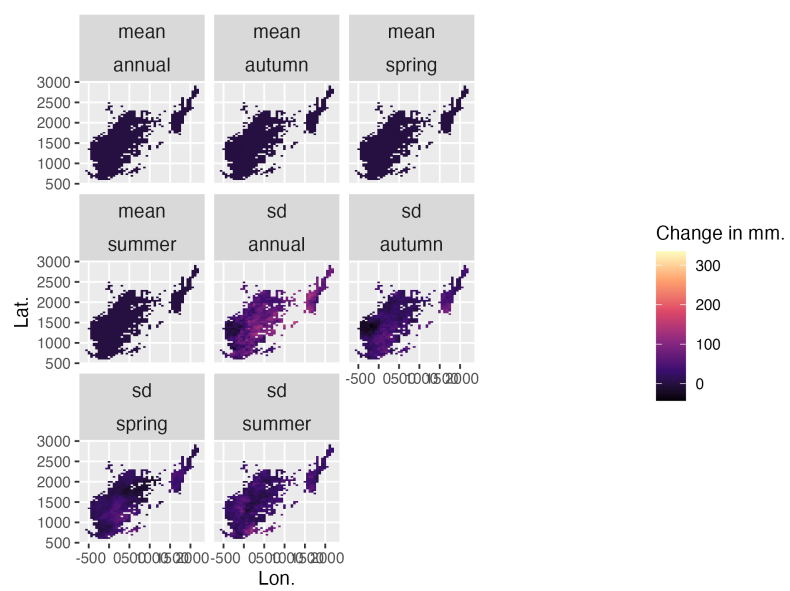


Figure A15: **Change in seasonal climate variables between the periods 1895-1925 and 1990-2020 across the distribution of *E. virginicus*.** Color represents change in (A) seasonal temperature (°C) and (B) seasonal precipitation (mm.). Maps show pixels covering the modeled distribution of *E. virginicus* used in *post hoc* climate regression analysis.

Table A1: Summary of herbarium samples across collections (no. of specimens)

Herbarium Collection	<i>A. hyemalis</i>	<i>A. perennans</i>	<i>E. virginicus</i>
Botanical Research Institute of Texas	350	190	198
Louisiana State University	72	38	62
Mercer Botanic Garden	3	0	6
Missouri Botanic Garden	210	205	122
Texas A&M	100	0	72
University of Kansas	134	34	197
University of Oklahoma	85	34	95
University of Texas & Lundell	183	91	102
Oklahoma State University	51	10	74

1094

Supporting Methods

1095

ODMAP Protocol

1096 [Overview](#)

1097 **Model purpose:** Mapping current distribution of *Epichloë* host species.

1098 **Target species:** *Agrostis hyemalis*, *Agrostis perennans*, and *Elymus virginicus*.

1099 **Study area:** Eastern North America

1100 **Spatial extent:** -125.0208, -66.47917, 24.0625, 49.9375 (xmin, xmax, ymin, ymax).

1101 **Spatial resolution:** 0.04166667, 0.04166667 (x, y).

1102 **Temporal extent:** 1990 to 2020.

1103 **Boundary:** Natural.

1104 [Data](#)

1105 **Observation type:** Occurrence records from Global Biodiversity Information Facility and

1106 herbarium collection across eastern North America. We used 713 occurrences records for *Agrostis*
1107 *hyemalis*, 656 occurrence records for *Agrostis perennans* and 2338 for *Elymus virginicus*.

1108 **Response data type:** occurrence record, presence-only.

1109 **Coordinate reference system:** WGS84 coordinate reference system (EPSG:4326 code)

1110 **Climatic data:** raster data extracted from PRISM; 30-year normal mean and standard deviation
1111 of temperature and of precipitation for three four-month seasons within the year (Spring: January,
1112 February, March, April; Summer: May, June, July, August; Autumn: September, October,
1113 November, December).

1114 **Model**

1115 **Model assumption:** We assumed that the target species are at equilibrium with their environ-
1116 ment.

1117 **Algorithms:** Maximum entropy (maxent)

1118 **Workflow:** We described the workflow in the methods section of the manuscript.

1119 **Software:** All statistics were performed using Maxent 3.3.4 and R4.3.1 with packages terra, usdm,
1120 spThin and dismo.

1121 **Code availability:** Available through this link: <https://github.com/joshuacfowler/EndoHerbarium>

1122 **Data availability:** Data was accessed through open-source R packages *rgbif*. *A. hyemalis*
1123 (GBIF.Org, 2025a), *A. perennans* (GBIF.Org, 2025b), *E. virginicus* (GBIF.Org, 2025c)

1124 **Assessment**

1125 We used AUC to test model performance.

1126 **Prediction**

1127 We predicted the probability of presence of the host species as a binary maps (presence or absence)

1128 *Mesh and Prior Sensitivity Analysis*

1129 To test the influence that the triangulation mesh and choice of priors has on results, we compared
1130 model results across a range of meshes and priors. We re-ran our model for the mesh used in main
1131 body of the text (Fig. A2), which we refer to as the "standard mesh", and with a mesh with smaller

minimum vertices (finer mesh). Finer scale meshes increase computation time. For each of these meshes, we ran the model with a range of priors defining the spatial range of our spatial random effects: 342km (the prior used for presented results), as well as ranges five times smaller (68 km) and five times larger (1714 km). We found generally that these choices did not alter the direction of model predictions, but did influence the associated uncertainty and magnitude of some effects.

For overall temporal trends, we found that models with differing priors predicted consistently positive relationships over time (Fig. A16).

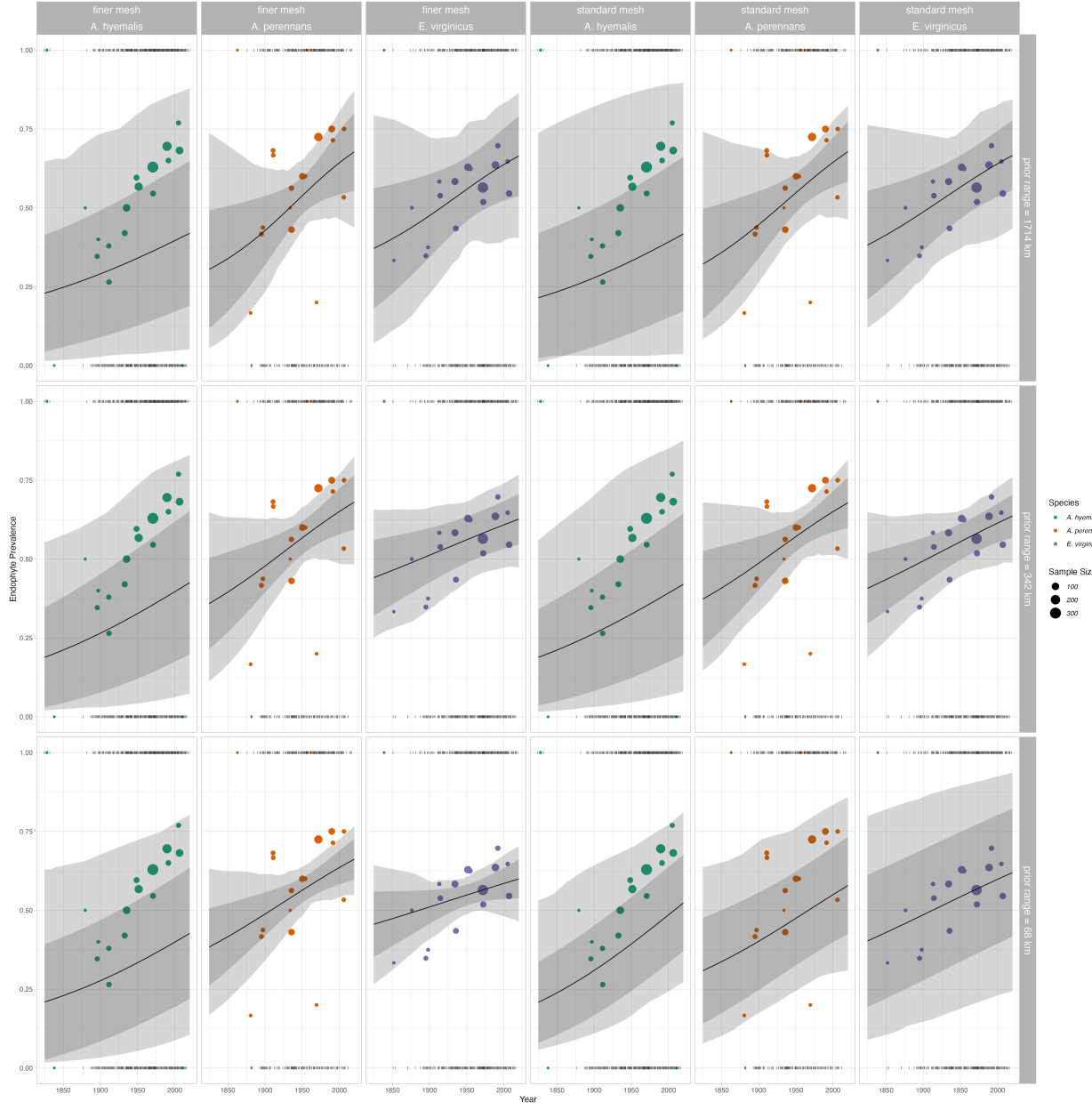


Figure A16: Overall trend in endophyte prevalence evaluated for endophyte prevalence models with different range priors on spatially structured random effects, and for two different triangulation meshes. Data used in model fitting is the same across all panels and as in the main text. Note that these plots, as compared to Fig. 2 in main text, show mean trends and do not incorporate variance associated with collector and scorer random effects.

1139 For spatially-varying temporal trends, we found that models with different priors predicted
1140 consistent spatial patterns in temporal trends, although the range of this prediction varied depending
1141 on the prior and mesh (Fig. A17 - A18). One noteworthy result of this analysis is that combinations
1142 of prior choice and mesh can introduce instability in model fitting. This is evident in A17 panel B
1143 and A18 panel B, where the prior range is smaller than the minimum vertex length of the mesh.
1144 Model fitting takes an extended time period and the model struggles to identify variation across
1145 space. Results with a set of prior ranges (Fig. A17 - A and C; Fig. A18 - A and C) result in
1146 models that estimate trends across space of the same direction and order of magnitude, although
1147 the "smoothness" of these predictions vary.

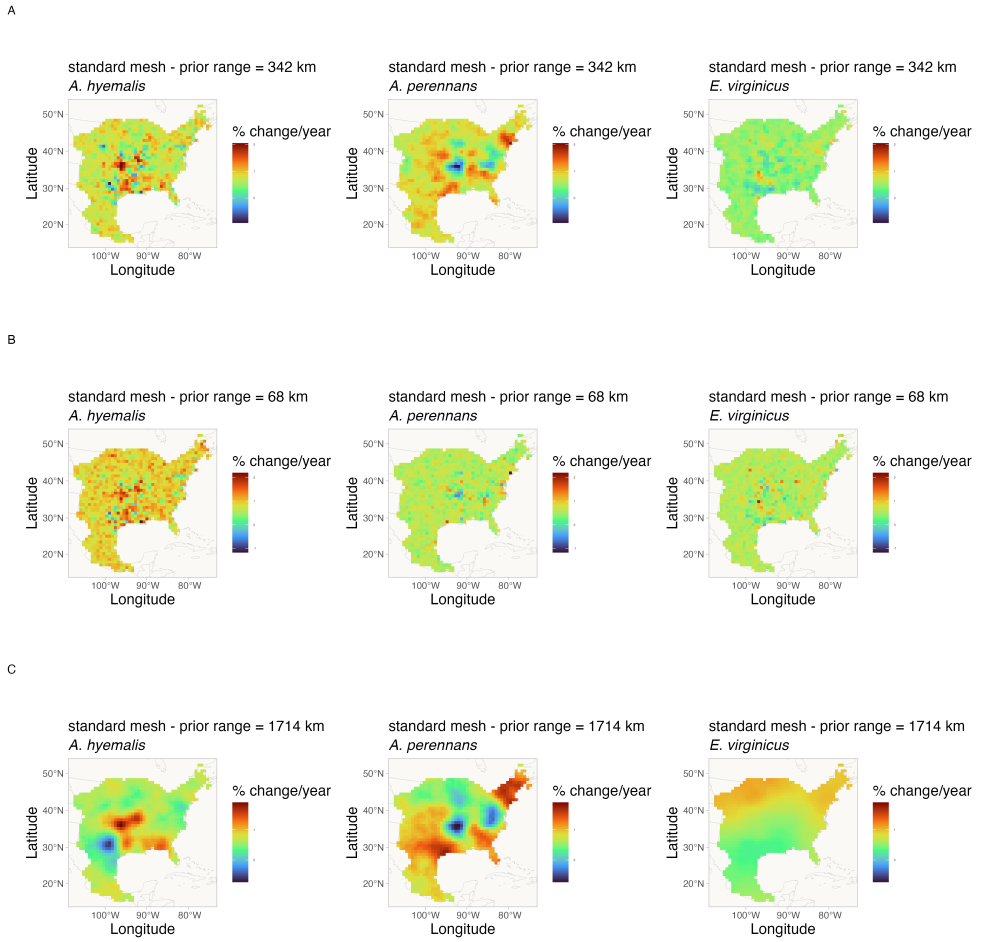
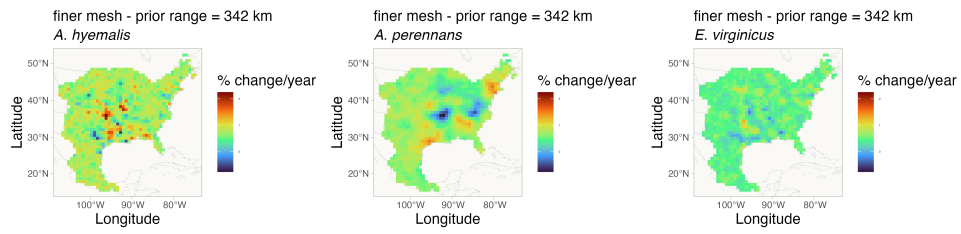
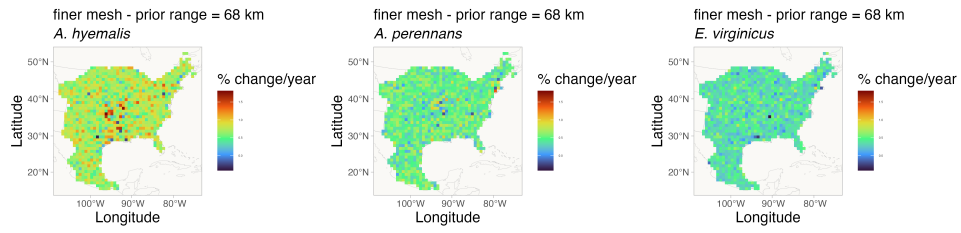


Figure A17: **Spatially-varying trends in endophyte prevalence evaluated for the endophyte prevalence model with different range priors on spatially structured random effects, and for the "standard" mesh.** Data used in model fitting is the same across all panels and as in the main text. Shading indicates the magnitude and direction of predicted trends for each of three host species for each of three prior ranges (rows A-C). Note that each plot has an individual scale bar.

A



B



C

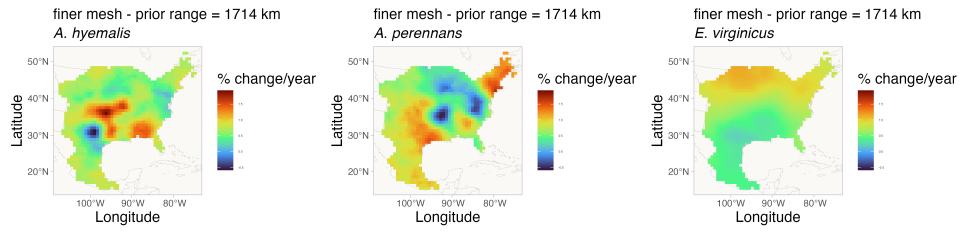


Figure A18: **Spatially-varying trends in endophyte prevalence evaluated for the endophyte prevalence model with different range priors on spatially structured random effects, and for the "finer" mesh.** Data used in model fitting is the same across all panels and as in the main text. Shading indicates the magnitude and direction of predicted trends for each of three host species for each of three prior ranges (rows A-C). Note that each plot has an individual scale bar.

1148

Spatially-biased Sample Size Simulation Analysis

1149 To examine how data that is unevenly distributed across host distributions may influence interpreta-
1150 tion of spatially-varying coefficients, we performed a simulation analysis. Our focal species, *Agrostis*
1151 *hyemalis*, *Agrostis perennans*, and *Elymus virginicus*, are widely distributed grasses across the east-
1152 ern United States that host *Epichloë* fungal endophytes. For logistical reasons, our sampling visits
1153 to herbaria focused on herbaria in the central southern U.S., which resulted in unevenly distributed
1154 data across each host species' range. This is particularly noteable for *Agrostis perennans* which has
1155 the most northern distribution and relatively fewer total collected specimens compared to the other
1156 focal species. Thus, a significant portion in the northeast of this species' range is relatively sparsely
1157 sampled. Our analysis presented in the main text identified this region as having strong increase in
1158 endophyte prevalence. Future visits to herbaria with regional focuses in the Northeastern US would
1159 certainly garner new specimens that could provide valuable insights into shifting host and symbiont
1160 distributions.

1161 *Simulation of spatially-biased symbiont occurrence data*

1162 We simulated datasets with varying levels of missing-ness to examine how this missing-ness influ-
1163 enced the estimation of spatially-varying trend estimates. We first generated 300 data points for
1164 each of three hypothetical species at random positions across an area approximating the scale of
1165 our focal data. Each data point was randomly assigned a year of collection across 200 years. We
1166 then simulated data from a Bernoulli process with trends alternating across nine regions (Fig. A19)
1167 in a 3X3 grid pattern. This grid pattern was intended to create a complex spatial layout of trends,
1168 where trends were either an increase of 1% per year or a decrease of 1% per year.

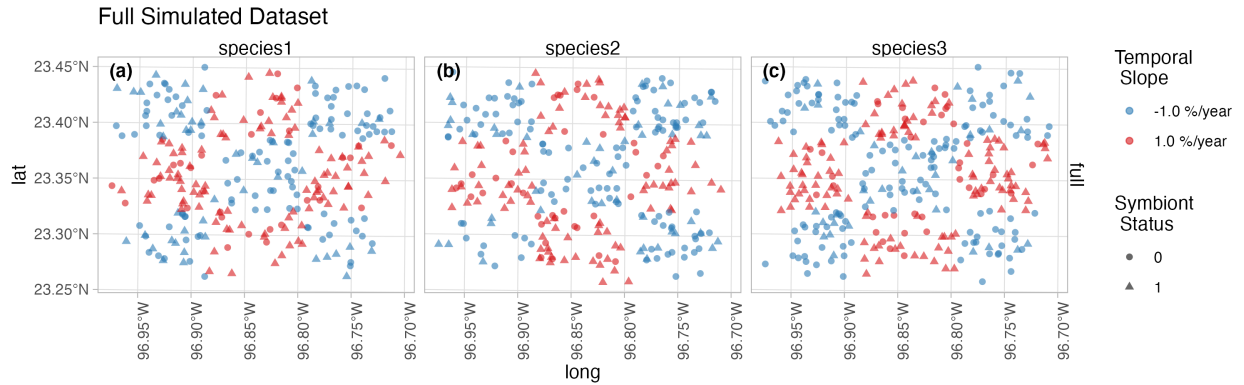


Figure A19: **Full simulated dataset of symbiotic association with spatially-varying temporal trends.** Color indicates the slope parameter used to simulate trends in endophyte status across nine "regions" for three species. Data are assigned collection years across a period of 200 years. Shape indicates the presence (1) or absence (0) of a symbiont.

1169 From this full data, we generated six additional datasets with missing-ness in the northeast
 1170 region of the simulated data for hypothetical species 2. The data remained the same for Species 1
 1171 and for species 3 across all datasets. For these six datasets, we removed data points at random in
 1172 six ways: 0% of datapoints in northeast region, 0% of recent datapoints, only 20% of datapoints,
 1173 only 20% of recent datapoints, only 50% of datapoints, and only 50% of recent datapoints (Fig.
 1174 A20). We define the datapoints as part of the recent time period if they occur later than the median
 1175 year. The result is 6 scenarios exploring degrees of spatial and temporal bias.

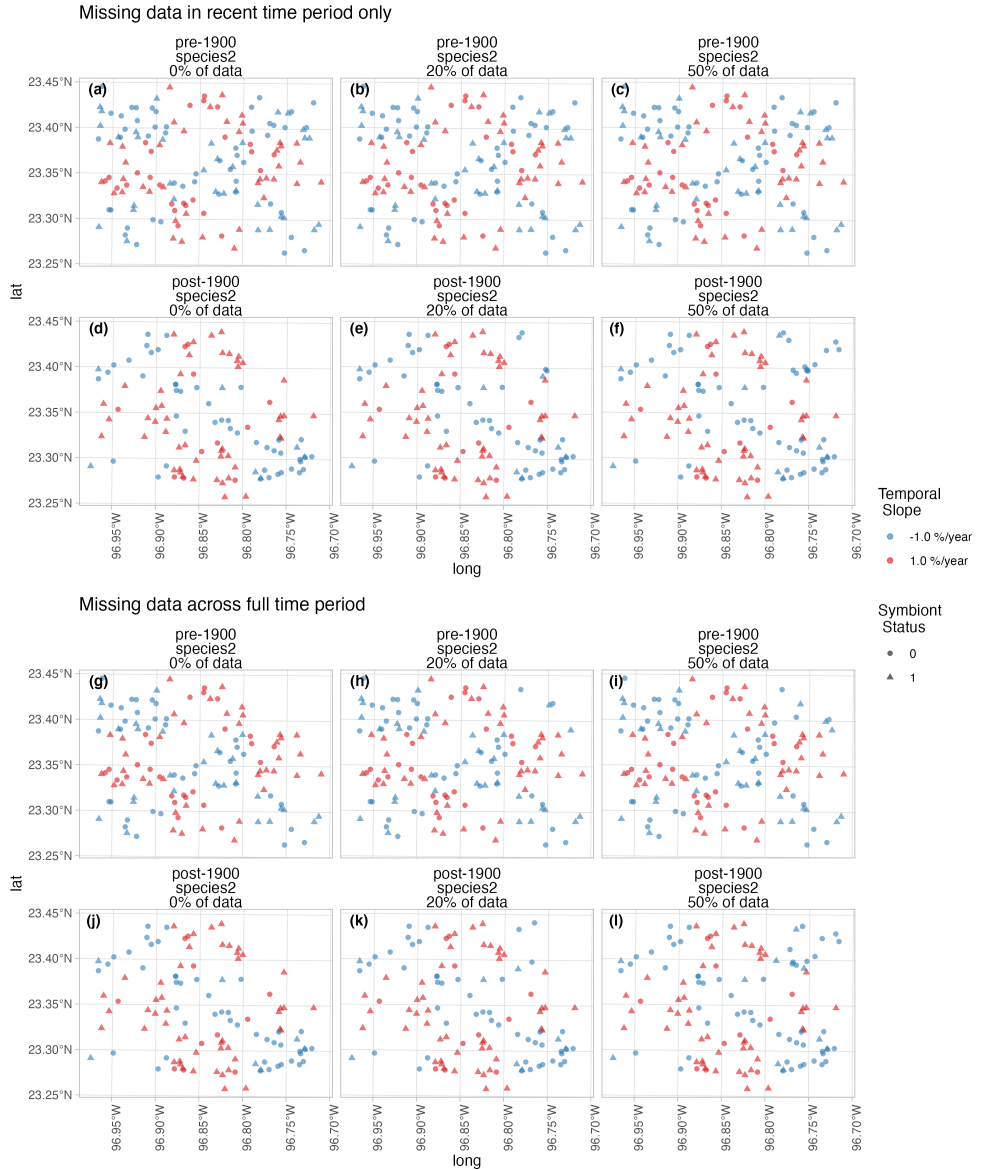


Figure A20: Six simulated datasets representing scenarios of spatially-baised missingness for Species 2. Missingness was imposed in the northeast region for six scenarios: 0% of recent datapoints available (a,d); only 20% of recent datapoints (b,e); only 50% of recent datapoints (c,f); 0% of datapoints across the full time period available (g,j); only 20% of datapoints across the full time period (h,k); and only 50% of datapoints across the full time period(i,l). Missingness was imposed only for hypothetical Species 2; Species 1 and 3 remain as in Figure A19. Color indicates the slope parameter used to simulate trends in endophyte status across 9 regions in a 3x3 grid. Shape indicates the presence (1) or absence (0) of a symbiont.

1176 *Statistical analysis*

1177 We analyzed each dataset with a model given by Eqn. A1 similar in construction to that used in
1178 our central analysis.

$$\text{logit}(\hat{P}_{h,i}) = A_h + T_h * \text{year}_i + \alpha_{h,l_i} + \tau_{h,l_i} * \text{year}_i + \delta_{l_i} \quad (\text{A1})$$

1179 Where symbiont presence/absence of the i^{th} specimen ($P_{h,i}$) was modeled as a Bernoulli re-
1180 sponse variable with expected probability of symbiont occurrence $\hat{P}_{h,i}$ for each host species h . We
1181 modeled $\hat{P}_{h,i}$ as a linear function of intercept A_h and slope T_h defining the global trend in endophyte
1182 prevalence specific to each host species as well as with spatially-varying intercepts α_{h,l_i} and slopes
1183 τ_{h,l_i} associated with location (l_i , the unique latitude-longitude combination of the i th observation).
1184 Similar to the SVC model of our central analysis (Eqn. 1), we estimated a shared variance term
1185 with the spatially-dependent random effect δ_{l_i} , intended to account for residual spatial variation.
1186 However in this analysis we omit i.i.d.-random effects terms associated with collector and scorer
1187 identity (χ_{c_i} and ω_{s_i} in Eqn. 1) for the sake of simplicity.

1188 *Influence of spatially-biased sampling on model interpretation*

1189 Our analysis of the full simulated data shows that our model is suitably flexible to capture complex
1190 spatial patterns in temporal trends (Fig. A21 a-c). Beyond this, the model also qualitatively
1191 captures the spatial patterns in temporal trends even with large amounts of data missingness (i.e
1192 missing up to 80% of the datapoints (Fig. A21 p-r)).

1193 While this analysis is not an exhaustive examination of the influence of sampling bias on our
1194 results for several reasons (including not examining how different strengths in temporal trends,
1195 different spatial arrangements of missing-ness influence model estimates, or different sample sizes
1196 influence results), it demonstrates that the spatially-varying modelling framework implemented in
1197 INLA we employ can suitably recover regional trends even with significant spatially-bias within
1198 data collection, and further the analysis is likely robust to temporally-structured bias (missing data

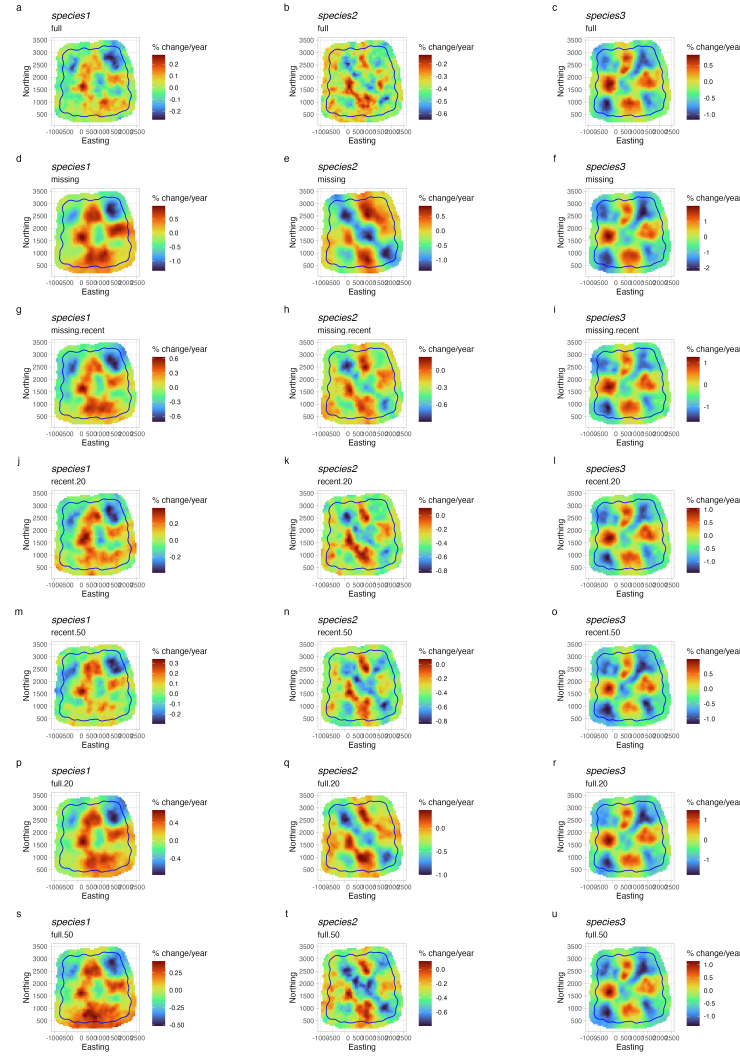


Figure A21: Mean predicted spatially-varying trend in symbiont prevalence across datasets with different levels of missingness. Color indicates the estimated mean temporal trend within each pixel across the simulated data. Panels show estimates for models fit to different levels of missing data for species 2 in the northeast region ((a-c) the full dataset, (d-f) missing all datapoints across entire temporal period, (g-i) missing all datapoints only during the recent period, (j-l) missing 80% of the datapoints only during the recent period, (m-o) missing 50% of the datapoints only during the recent period, (p-r) missing 80% of the datapoints across the entire temporal period, (s-u) missing 50% of the datapoints across the entire temporal period). The mesh boundary that bounds the "full" simulated dataset is plotted in each panel.

1199 within recent collection period). Future work could more fully explore the scenarios that cause
1200 this ability to break down. We expect this simulation reflects what may be a common scenario for
1201 research investigating global change using natural history specimens. Collection effort by trained
1202 taxonomists and professional collectors peaked in the past, and collections contain relatively fewer
1203 modern specimens in many regions. Additionally, most global change research necessarily involves
1204 accessing many specimens across collections. Research efforts such as ours will be unable to access
1205 every specimen from all possible collections. Ongoing digitization efforts will make it possible to
1206 more clearly assess how much data is missing from a particular study compared to the actual
1207 holdings of natural history collections, but ultimately, the decision of what data and collections to
1208 include is a question of sample size and study design.